Sathia Ramalingam[1], Vijayalakshmi Ramalingam[2], Aswin Sriram[2]*

[1]Department of Civil Engineering, Sri Venkateswara College of Engineering, Chennai, [2]Department of Civil Engineering, Sri Sivasubramaniya Nadar College of Engineering, Kalavakkam, Chennai – 603110

Scientificpaper
ISSN 0351-9465, E-ISSN 2466-2585
https://doi.org/10.62638/ZasMat1420

Zastita Materijala 67 ()
(2026)

Optimization of alkali-activated fly ash-based geopolymer mortar: Influence of activator composition on strength and workability

ABSTRACT

The influence of alkali activator composition, water content, and mix proportions on the fresh-state workability, mechanical properties, and microstructure of fly ash-based geopolymer mortars is investigated in this study. A total of 40 geopolymer mortar mixes were prepared, and three replicate specimens were tested for each mix. All mixes were produced with a constant sand-to-fly ash ratio of 2:1, while the sodium hydroxide (NaOH) molarity was varied at 8 M, 12 M, 14 M, and 16 M, and the sodium silicate-to-NaOH (SS/NaOH) ratio ranged from 0.1 to 2.5. The water content was varied from 1 to 8% by weight of fly ash for fixed solution-to-binder ratios of 0.4 and 0.5. The samples were cured at 85°C for 24 hours in an oven to aid geopolymerization. Workability was evaluated using the flow table test, and flow values ranged between 120% and 140%. Compressive strength was determined at curing ages of 3, 7, and 28 days. The maximum compressive strength of 68 MPa was obtained at a NaOH concentration of 16 M and an SS/NaOH ratio of 1.5. This optimum composition corresponds to a Na_2O/SiO_2 ratio in the range of 0.15–0.17, indicating that both parameters describe the same optimum activator chemistry expressed using different ratio formats. X-ray diffraction (XRD) analysis revealed the formation of hydroxysodalite-type zeolite phases at higher SS/NaOH ratios, contributing to enhanced strength development. An increase in the H_2O/Na_2O ratio beyond 0.22 resulted in reduced strength due to increased porosity. The results identify critical activator and water-content ranges that enable an effective balance between workability and compressive strength, providing a quantitative basis for mix proportion optimization of fly ash-based alkali-activated mortars.

Keywords: *Geopolymer mortar. Alkali activation, Compressive strength, Rheology and workability, Phase transformation*

1. INTRODUCTION

Sustainable construction materials have created a huge interest among the construction industry and amongst the researchers [1,2]. Geopolymer mortars are being considered as alternatives to Portland cement-based systems Geopolymers are flexible binders produced from aluminosilicates in the presence of alkaline activators [3,4]. They offer superior mechanical properties as well as better durability. The use of industrial by-products such as fly ash in geopolymer mortars helps to achieve desirable strength and durability for reinforced cement concrete (RCC) structure [5,6]. Geopolymer mortars are eco-friendly and durable alternatives to ordinary mortars [7,8].

However, their characteristics highly depend on the composition of the precursor, activator concentration, and curing conditions [9,10]. Therefore, understanding their mechanical properties and fresh-state workability is important.The basic geopolymerization reaction includes the dissolution of alumina and silica from precursor materials under alkaline conditions followed by polycondensation forming a rigid 3D network [11].The effectiveness of this process depends on several parameters or factors which includes sodium hydroxide (NaOH) molarity, sodium silicate to NaOH ratio and water to activator ratio which governs the microstructure and properties of hardened matrix [12,13]. While NaOH helps dissolve the aluminosilicate species, sodium silicate provides polymerization kinetics as well as binding ability which reinforces geopolymer gel [14,15]. Yet, use of more NaOH will cause viscosity to be so high which can impair workability, while unbalance of activator ratios will hamper strength development [16,17]. The Si/Al ratio of fly ash–based geopolymer systems plays a significant role

*Corresponding author: Vijayalakshmi Ramalingam
E-mail: vijayalakshmir@ssn.edu.in
Paper received: 29.01.2025.
Paper corrected: 25. 02. 2026.
Paper accepted: 08.03.2026.

in determining the reaction products and the compactness of the resulting microstructure [18,19].

Although several studies have investigated the influence of alkali activator concentration and curing conditions on geopolymer mortars, most investigations have focused primarily on either mechanical performance or fresh-state behaviour independently [20,21]. Limited studies have attempted to establish a systematic relationship between activator chemistry, water content, and phase evolution governing both workability and strength development simultaneously [22,23]. In particular, the combined influence of NaOH molarity, sodium silicate-to-sodium hydroxide ratio, and water-to-sodium oxide ratio on the geopolymerization kinetics and microstructural transformation remains insufficiently quantified [24,25]. As a result, the identification of optimal activator composition ranges that ensure both adequate workability and enhanced mechanical performance remains a challenge for practical applications.

A significant challenge related to geopolymer technology is optimizing workability and compressive strength especially in fly ash-based system [26,27]. The flow properties of geopolymer mortars are governed by the rheology of the paste at the fresh state, the liquid-to-binder ratio and activator concentration activated superplasticizer content of the binder [28,29]. Raising water content increases flowability, but can raise porosity and reduce strength. On the other hand, lower water-to-binder ratios lead to more compact packing density and long-term strength retention but reduce workability, which calls for superplasticizers [30,31]. Studies show that the right sodium silicate-to-NaOH ratio helps in balancing workability and mechanical properties in geopolymer mortars to produce a workable and high-strength material [32,33]. The compressive strength of geopolymer mortars is immensely affected by the curing regime that alters reaction kinetics and final microstructural properties [34,35]. High curing temperatures boost geopolymer activity and early strength but can cause shrinkage and cracking with excessive heat [36,37]. The ratio of Na_2O/SiO_2 is another important factor affecting strength development as it controls the availability of reactive silica for gel formation [38,39]. Research shows that a well-optimized Na_2O/SiO_2 ratio helps polymerization and densification, giving it a higher load-bearing capacity [40,41]. Furthermore, geopolymer systems can form secondary crystalline phases like zeolites and hydroxysodalite [42,43]. These secondary phases can result in geopolymer systems that are durable in the long-run [44,45]. However, they can also result in low early-age strength depending on the mix proportions and activator dosages [46,47,48].

The durability and long-term performance of geopolymer mortars are crucial for their success as a sustainable alternative to conventional cement-based materials[49]; [50]. The amount of spaces in geopolymer matrices plays an important role in their interfacing with the environment[51]; [52]. Also, more water may lead to more porosity which may affect the durability. Research has shown that, a lower water to activator ratio can result in less voids enabling resistance to chemicals and freeze thaw cycles[53]; [54]. The study also highlights the significance of having the proper mix proportions to assist in the completion of polymerization reactions and the initiation of secondary polymerization reactions[55]; [56]. Durability-related aspects such as porosity and moisture transport are known to influence the long-term performance of geopolymer mortars in real-world applications[57]; [58].

2. NEED FOR PRESENT INVESTIGATION AND NOVELTY OF RESEARCH

Furthermore, previous studies have reported that excessive alkali concentration or water addition may lead to incomplete polymerization, formation of secondary crystalline phases, and increased porosity, ultimately affecting long-term strength development[59];[60]. However, the interaction between Na_2O/SiO_2 ratio and H_2O/Na_2O ratio under controlled solution-to-binder conditions has not been extensively examined in fly ash–based geopolymer mortars. Establishing these relationships is essential for developing reliable mix proportioning strategies that can translate laboratory-scale geopolymer formulations into field applications while maintaining consistent rheological and mechanical performance.

Due to increasing interest in geopolymer technology for sustainable construction, this study conducts systematic investigations on the effect of important mix parameters. In this regard, workability, compressive strength and microstructure development of fly ash geopolymer mortar was ascertained. In this study, ‘water content’ refers to the percentage of added water by weight of fly ash, while the ‘water-to-activator ratio’ denotes the ratio of total water to alkaline activator solution.Here the current study critically examines how the molarity of NaOH, sodium silicate-to-NaOH ratio, water-to-activator ratio and precursor composition are correlated to processing conditions and mechanical performance. The research also examines how water content affects strength development and finds ideal mixtures that optimize performance in the fresh state and after curing. The

research assesses the flow behaviour, compressive strength, and phase composition of different geo-polymer mortar mix designs to optimize and improve the existing sustainable binder technologies.

The novelty of the present study lies in the systematic integration of activator chemistry, water content, and microstructural evolution to establish quantitative relationships governing both fresh-state workability and compressive strength development in fly ash–based geopolymer mortars. Unlike previous studies that evaluate activator parameters independently, this research correlates NaOH molarity, SS/NaOH ratio, Na_2O/SiO_2 ratio, and H_2O/Na_2O ratio within controlled solution-to-binder systems to identify optimal ranges for geopolymerization efficiency. The study further combines experimental observations with phase characterization and mathematical modelling to develop predictive relationships for strength evolution, thereby providing a unified framework for mix proportion optimization of geopolymer mortars suitable for sustainable construction applications.

3. MATERIALS AND METHODS

The geopolymerization process is influenced by many factors, including the composition of the precursor, molarity and type of alkali activator, curing condition, and mix proportioning[61]; [62]. The study examines the effect of different compositions of activators on mechanical properties of geopolymer mortar so as to optimize the compressive strength. The experimental program was designed to systematically assess the effects of sodium silicate, Na_2SiO_3, to sodium hydroxide, NaOH, ratio, NaOH molarity and solution-to-binder, S/B, ratio on geopolymeric bond formation. The main ingredients used for the preparation of geopolymer mortar are Class F fly ash and river sand as fine aggregate[63]; [64]. The fly ash was collected from the electrostatic precipitators in dry form. The SiO_2/Al_2O_3 ratio was about 2, which classified it as low calcium fly ash per ASTM C618:2005. Silica fume, a secondary pozzolanic material, has SiO_2 content of approximately 82% which adds to the reactivity of the geopolymer[65]; . The Na2SiO3 solution is 28% SiO_2, 8% Na_2O and 64% water specific gravity 1.48 g/cm^3. The NaOH solution used is prepared at 8M, 12M, 14M and 16M concentrations. The day before mixing, NaOH pellets were added to distilled water to create the NaOH solution[66]. The mass of solid NaOH required varies with molarity, or concentration. The 8M solution has 26.2% NaOH solids while the 16M solution has 44.4%. Fine aggregate was River sand which was graded and sieved through 2.36 mm sieve. The superplasticizer dosage was kept within a limited range and was not treated as an independent variable in the experimental program[67].

The mortar mix ratios have been designed with a constant sand-to-fly-ash ratio of 2:1 and varying the S/B ratios. 0.4 and 0.5. The ratio of SS/NaOH was varied between 0.1, 0.2, 0.5, 1.5 and 2.5 for studying its effect on geopolymerization. The new mortar flowability was controlled by keeping it within the limit of 130 ± 10%. A Hobart mixer with a 5-liter capacity was used for mixing at ambient temperature (28°C). First, fly ash and activator solution (Na_2SiO_3 + NaOH) were mixed for 3 min which was followed by addition of sand and mixing continued for additional 3 min. If required, a pre-determined and limited amount of superplasticizer or additional water was added only to achieve the target flowability range of 130 ± 10%, while keeping the solution-to-binder ratio fixed, and mixing was continued at low speed (60 RPM) for a further 3 minutes. Workability was tested for the mixture by conducting a flow table test, in this test, the mortar was compacted in a truncated cone mold, to this mold 25 jolts were given in 15 seconds and average of three diameter measurements taken, this average is designated as flow diameter. For each mix, three cube specimens were cast and tested at each curing age, and the reported compressive strength values represent the average of three specimens (n = 3). The samples were cured at 85°C for 24 hours in an oven to aid geopolymerization so that sufficient polymeric bond could be formed. After curing, the samples were stored under ambient conditions, and compressive strength tests were conducted at 3, 7, and 28 days using a 2000 kN compression testing machine. The average values are reported, and the experimental variability was within acceptable limits. The compressive strength peaked at 68 MPa with a Na2O/SiO2 ratio of 0.15–0.17. Strength declined due to supersaturation, which limited the extent of geopolymerization. The use of X-ray Diffraction (XRD) analysis was performed to characterize the phase of the hardened geopolymer mortar. The powdered samples were subjected to phase characterization through XRD analysis using a Shimadzu X-ray Diffractometer (CuKα radiation, λ = 1.5405 Å) by sieving them on a 75 μm sieve. Operating conditions were set to have a 2θ range between 7 and 50 (0.1°/s step size). Scanning Electron Microscopy (SEM) analysis was carried out to examine the microstructural features and morphology of the hardened geopolymer mortar samples, focusing on gel formation, pore structure, and matrix densification. The mix proportion of all the geopolymer mortar with solution to binder ratio of 0.4 and 0.5 is shown in Table 1 and Table 2 respectively.

Table 1. Mix proportion of geopolymer Mortars with Solution to binder ratio of 0.4

S.No	FA (kg)	Solution/ /binder ratio	Sodium Silicate (SS)/ NaOH ratio	Sodium Silicate (SS) (kg)	NaOH (kg)	Molarity (M)	Extra Water (kg)	Mix H_2O/Na_2O ratio	Mix Na_2O/SiO_2 ratio
1	1	0.4	0.1	0.036	0.36	8	0	12.97	0.16
2	1	0.4	0.2	0.067	0.33	8	0	13.38	0.15
3	1	0.4	0.5	0.133	0.27	8	0.012	14.45	0.13
4	1	0.4	1.5	0.24	0.16	8	0.031	16.79	0.1
5	1	0.4	2.5	0.286	0.11	8	0.041	18.16	0.09
6	1	0.4	0.1	0.036	0.36	12	0.011	9.1	0.21
7	1	0.4	0.2	0.067	0.33	12	0.022	9.53	0.2
8	1	0.4	0.5	0.133	0.27	12	0.03	10.7	0.17
9	1	0.4	1.5	0.24	0.16	12	0.045	13.48	0.12
10	1	0.4	2.5	0.286	0.11	12	0.06	15.26	0.1
11	1	0.4	0.1	0.036	0.36	14	0.017	7.68	0.24
12	1	0.4	0.2	0.067	0.33	14	0.026	8.11	0.22
13	1	0.4	0.5	0.133	0.27	14	0.039	9.26	0.18
14	1	0.4	1.5	0.24	0.16	14	0.051	12.1	0.13
15	1	0.4	2.5	0.286	0.11	14	0.075	14.59	0.11
16	1	0.4	0.1	0.036	0.36	16	0.034	6.74	0.26
17	1	0.4	0.2	0.067	0.33	16	0.041	7.16	0.24
18	1	0.4	0.5	0.133	0.27	16	0.058	8.29	0.2
19	1	0.4	1.5	0.24	0.16	16	0.077	10.25	0.21
20	1	0.4	2.5	0.286	0.11	16	0.081	11.25	0.2

Table 2 Mix proportion of geopolymer Mortars with Solution to binder ratio of 0.5

S.No	FA (kg)	Solution /binder ratio	Sodium Silicate (SS)/ NaOH ratio	Sodium Silicate (SS) (kg)	NaOH (kg)	Molarity (M)	Superplasticizer (SP) (% of FA)	Extra Water (kg)	Mix H_2O/Na_2O ratio	Mix Na_2O/SiO_2 ratio
1	1	0.5	0.1	0.045	0.45	8	0	-	10.35	0.17
2	1	0.5	0.2	0.083	0.42	8	0.3	-	10.75	0.15
3	1	0.5	0.5	0.167	0.33	8	0.8	-	12.26	0.13
4	1	0.5	1.5	0.3	0.2	8	1.2	-	15.81	0.1
5	1	0.5	2.5	0.357	0.14	8	1.4	-	18.14	0.08
6	1	0.5	0.1	0.045	0.45	12	0	-	7.58	0.22
7	1	0.5	0.2	0.083	0.42	12	0.7	-	8.27	0.2
8	1	0.5	0.5	0.167	0.33	12	1.2	-	9.64	0.17
9	1	0.5	1.5	0.3	0.2	12	1.7	-	13.19	0.12
10	1	0.5	2.5	0.357	0.14	12	2	-	16.03	0.1
11	1	0.5	0.1	0.045	0.45	14	0	-	6.58	0.25
12	1	0.5	0.2	0.083	0.42	14	1	-	7.17	0.23
13	1	0.5	0.5	0.167	0.33	14	1.4	-	8.27	0.19
14	1	0.5	1.5	0.3	0.2	14	1.6	-	11.24	0.16
15	1	0.5	2.5	0.357	0.14	14	2	0.014	14.22	0.11
16	1	0.5	0.1	0.045	0.45	16	0	-	5.47	0.27
17	1	0.5	0.2	0.083	0.42	16	1.5	-	6.7	0.25
18	1	0.5	0.5	0.167	0.33	16	1.7	-	8.24	0.2
19	1	0.5	1.5	0.3	0.2	16	2	0.014	12.03	0.17
20	1	0.5	2.5	0.357	0.14	16	2	0.022	14.6	0.11

4. RESULTS AND DISCUSSION

4.1. Phase and Microstructural Characterization

4.1.1. Spectral – XRD analysis

The geopolymer mortar showed the XRD patterns over a 2θ range of 7° to 50° at a scanning rate of 0.1°/second. The peak of the geopolymer mortar diffraction pattern (Fig. 1) is at 2θ=26.9 °, which is the highest. The peak lesser to this is at 2θ=21.1°. Comparatively, the geopolymer mortar shows a reduction in amorphous hump compared to the XRD pattern of unreacted fly ash showing formation of new reaction product[25]. The XRD pattern for the unreacted fly ash shows the presence of mainly an amorphous glassy phase along with a few crystalline phases like quartz (SiO_2), magnetite (Fe_3O_4), and mullite ($Al_6Si_2O_{13}$). The appearing of new diffraction peaks and broadening of patterns in geopolymer mortar indicates phase transformation involvement caused by reaction products [68]. According to the XRD results, the geopolymer mortar produces zeolite phases, particularly the formation of hydroxy sodalite ($Na_6(AlO_2)_6(SiO_2)_{10}\cdot 12H_2O$) [69]. The direct identification of the characteristic peaks corresponding to hydroxysodalite at 2θ = 9.88°, 11.19°, 22.36°, 22.49°, and 26.04°. Out of all the mortars, the one with 16M NaOH and SS/NaOH ratio of 1.5, i.e., 16GM1.5 shown on intensity peaks of highest value specifying the formation of crystalline geopolymer. This is similar to other studies that show that the soluble silica in the activator solution is critical for forming zeolite [70].

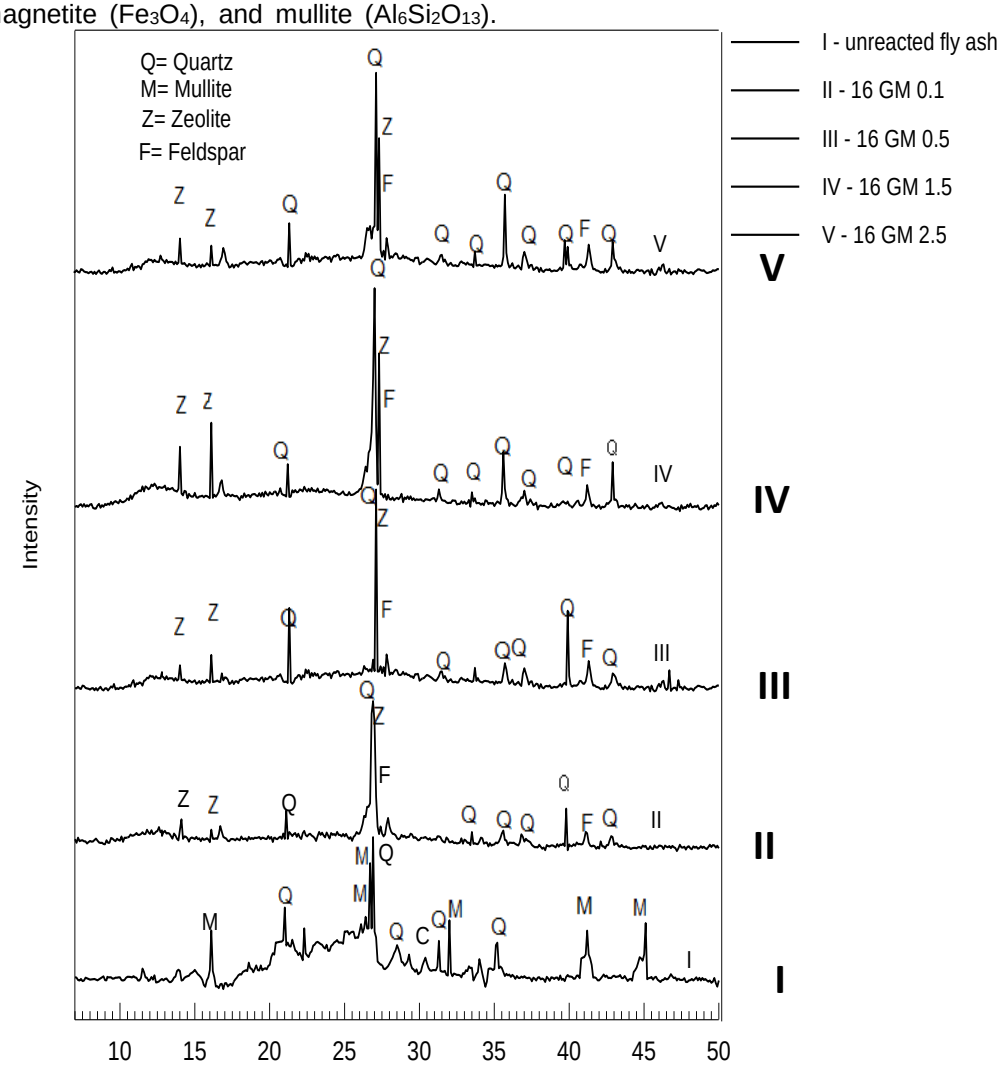

Figure 1. XRD patterns of unreacted fly ash and geopolymer mortars with 16 M NaOH at different SS/NaOH ratios: (I) unreacted fly ash, (II) 16GM–0.1, (III) 16GM–0.5, (IV) 16GM–1.5, and (V) 16GM–2.5.

The comparative XRD patterns of mortars with different SS/NaOH ratios (from 0.1 to 2.5) indicate that as SS/NaOH increases, the peak intensities of hydroxysodalite become higher. Higher soluble silica concentrations enhance polymerization, thus promoting crystalline geopolymeric structure

development. However, When the SS/NaOH ratio more than than 1.5 any further addition of Na_2SiO_3 did not improve crystallinity significantly, thereby indicating that it is not being added to the product of reaction. At SS/NaOH = 1.5, the system reaches adequate supersaturation contributing to the formation of well-ordered precipitated gels [49]. The analyses obtained through XRD confirm that the amorphous phase of fly ash has been transformed into that of a geopolymer, which is further confirmed by the success of zeolization, a major indicator of geopolymerization [71]. The outcomes emphasize that the extent of polymerization and crystallinity depends on the NaOH molarity and SS/NaOH ratio significantly.

The strength development observed in the present study can be directly correlated with the phase evolution identified from the XRD patterns [72]. Previous studies have reported that the formation of amorphous aluminosilicate gel phases, primarily N–A–S–H and C–(N)–A–S–H type gels, plays a dominant role in improving the mechanical performance of geopolymer mortars by producing a dense and continuous binding matrix [73]. The increase in compressive strength with optimized activator composition is attributed to enhanced dissolution of reactive silica and alumina species, followed by polycondensation reactions leading to the formation of stable geopolymeric gels [74]. Similar observations were reported in fly ash–based geopolymer systems where improved strength was associated with increased amorphous phase content and refined microstructure due to enhanced gel formation [11].

Furthermore, the reduction in unreacted crystalline phases and the increased intensity of reaction products observed in the XRD spectra indicate improved geopolymerization efficiency, resulting in reduced porosity and improved inter-particle bonding [75]. Studies on geopolymer mortars incorporating industrial by-products have shown that optimal alkali activation promotes the formation of hybrid gel systems such as N–A–S–H and C–A–S–H, which contribute to higher compressive strength through matrix densification and improved load transfer mechanisms [76,77].

The relationship between microstructural evolution and strength development has also been confirmed in geopolymer systems subjected to different curing and compositional conditions, where the increase in gel formation and reduction of microcracks were associated with improved mechanical performance [78]. XRD-based phase transformation analysis has demonstrated that the development of a compact aluminosilicate network significantly enhances strength by limiting pore connectivity and improving structural integrity [79]; [80].

4.1.2. Microstructural Analysis

The SEM raw materials used for this study is shown in Fig. 2. The SEM micrograph in Fig.3(a) corresponds to a geopolymer mortar synthesized with 8 M NaOH at a solution-to-binder ratio of 0.4, and SS/NaOH ratio of 0.1. The morphology clearly reveals a heterogeneous matrix with pronounced signs of structural discontinuities[74].

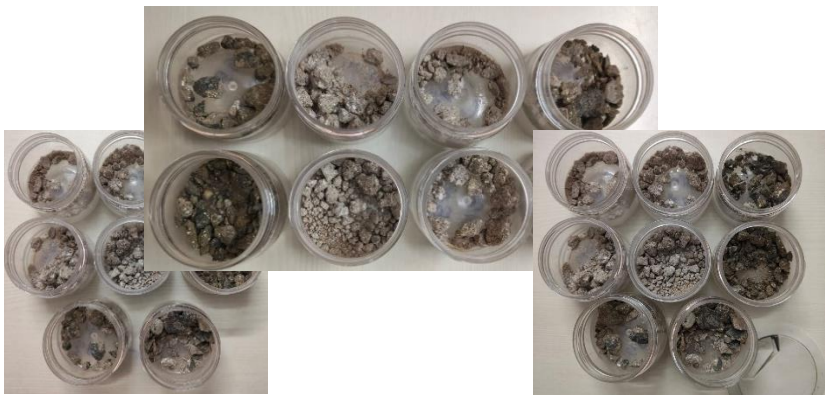

Figure 2. Geopolymer mortar samples used for SEM analysis

Multiple air voids and open pores are evident, suggesting insufficient densification during the geopolymerization process[69]. The presence of microcracks, shrinkage cracks, and debonded regions indicates sub-optimal gel formation and elevated internal stress development, possibly due to reduced dissolution rates at lower molarity [81]. Additionally, agglomerated gel clusters and fracture planes are distinctly visible, implying poor packing density and incomplete geopolymeric network

formation [14]. These morphological irregularities are consistent with the moderate compressive strength values (~12 MPa at 28 days) observed for this mix [68]. Furthermore, crack propagation paths and weak gel zones suggest that the microstructure lacks cohesive integrity, which aligns with XRD data indicating only partial formation of zeolitic crystalline phases, likely Na–A or Na–X type zeolites, in a dominantly amorphous matrix[82]. The low SS/NaOH ratio has contributed to limited silicate availability, impeding the growth of a robust N–A–S–H gel framework [83].

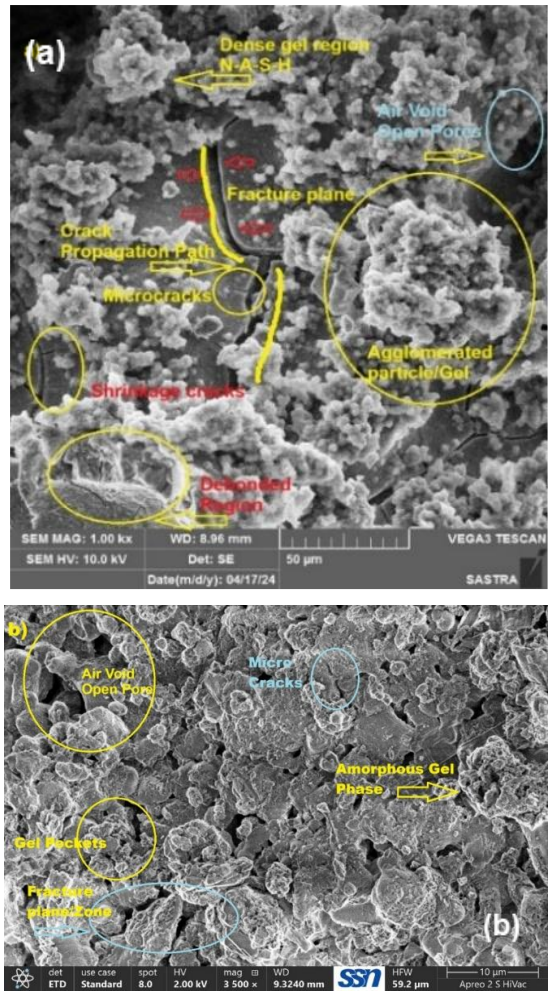

Figure 3 Microstructural Image (a) 8M, SS/NaOH ratio for solution /binder ratio of 0.4 and (b) 16M, SS/NaOH ratio for Solution / binder ratio of 0.5

Conversely, Fig.3(b) illustrates the micro structure of a geopolymer matrix synthesized using 16 M NaOH, solution-to-binder ratio of 0.5, and SS/NaOH ratio of 1.5—which corresponds to the optimized mix yielding 68 MPa at 28 days. The matrix exhibits a dense, homogeneously gelled structure with well-distributed amorphous gel phases, indicative of complete geopolymerization [70]. Only very fine microcracks and isolated air voids are visible, signifying high structural integrity and minimal shrinkage-induced damage[84]. The formation of gel pockets and a well-developed amorphous N–A–S–H matrix corroborates the high silicate availability at the optimized SS/NaOH ratio, which is further validated by XRD findings[85]. These spectra revealed intensified broad humps typical of highly amorphous aluminosilicate gels and enhanced intensity of zeolitic phases, indicating a significant degree of polycondensation [52]. The fracture zones in this image appear more cohesive, with no signs of propagation, confirming superior load-transfer capacity [44]. The microstructural refinement observed is thus a direct outcome of high alkaline concentration and balanced silicate content, leading to enhanced dissolution, polycondensation, and matrix densification [86].

4.2. Workability characteristics of Geopolymer Mortar

The properties of geopolymer mortar and its proportions affect its fresh properties like workability and consistency. The study maintained a sand-to-fly ash ratio of 2:1 and varied the solution-to-binder (S/B) ratios of 0.4 and 0.5 to study the flow and mechanical performance. Early tests using an S/B ratio of 0.35 were unsuccessful due to poor workability, needing very high SP and extra water for sufficient flow that may reduce strength of final geopolymer. So, S/B ratios of 0.4 and 0.5 were selected as favourable for subsequent assessment[76]. To assess the influence of the sodium hydroxide (NaOH) concentrated on workability, the NaOH molarity values were considered varying systematically 8M, 10M, 12M, 14M and 16M respectively. Moreover, the behaviour of sodium silicate was evaluated by adjusting its concentration from ratios of 0.1 to 2.5. An SS/NaOH ratio of less than 0.1 was found to be highly foamy, resulting in poor consistency and difficulties to place in the mould. This may have been due to insufficient polymeric interaction between the activator solution and the fly ash[82]; [87]. On the other hand, at SS/NaOH > 2.5, the mixtures were highly viscous and had difficulties with compaction and uniform dispersion of the reactants[88]. In order to achieve the target flow of 130 ± 10%, superplasticizer (0.5% to 2% by weight of fly ash) and extra water (1% to 8% by weight of fly ash) were added in a controlled manner. The changes made allowed for proper mixing of activator components while maintaining mix cohesion [63].

The viscosity of the activator solution controls the workability of the geopolymer mortar. In turn, the viscosity is controlled or depends on the concentration of NaOH and SS [31]. An increase in the molarity of NaOH from the 8M to 16M creates a decrease in workability of all mixes. This is due to the ionic concentration in the solution that

enhances the rate of dissolution of Si^{4+} and Al^{3+} species from fly ash leading to rapid gel formation [89]. Observation of the workability with SS/NaOH ratio revealed a similar trend in the opposite direction. Sodium silicate increases the overall silica content in the solution thereby increasing viscosity [52]. Studies carried out and reiterates this observation as they also found that higher NaOH and sodium silicate concentrations produced a paste that was denser and less workable due to rapid geopolymerization reaction. Attaining flowability-reactivity balance is important for the strength gain [58].

Without compromising the ease of placing the concrete. The use of superplasticizer can reduce the loss of workability, which means that mortars with higher concentration (14M and 16M) of NaOH have a flow that is still in the acceptable range[90]. As per the study requirement, some additional water was added in a few mixes, but excess water was avoided so as not to dilute the activator solution and hamper geopolymerization [91]. The workability results show that activator composition must be designed to produce a homogeneous geopolymer with good flowability and packing density [89]. Mix proportions with aggregate to binder ratio of 0.4 and 0.5 were found to be optimum based on workability and strength gain and can be selected for further examination in mechanical properties [54]. The next segment discusses how this mix proportions affect the flow behaviour and mechanical performance of geopolymer mortars, most particularly their compressive strength development over time.

4.3. Flow Characteristics of Geopolymer Mortars

The flow values reported in this study correspond to the adjusted flow measured after the addition of superplasticizer and/or controlled water adjustment to achieve workable mortar consistency suitable for casting. The initial flow prior to adjustment was observed to vary significantly depending on activator composition; however, the reported flow values represent the final measured flow used for comparison among mixes[89]. This approach was adopted to ensure consistent workability conditions while evaluating the influence of activator parameters on mechanical and microstructural performance [29].The flow values and the compressive strength for solution to binder ratio of 04.and 0.5 is listed in Table 3 and Table 4 respectively.

The ease of flow of geopolymer-based mortar is an important parameter influencing placement, compaction, and workability. To evaluate the flow characteristics of the geopolymer mortar mixes, the ASTM C1437-01 flow table test was performed. The mixes were targeted to a flow of 130 ± 10% to ensure an even spread in the moulds [56]. The findings reveal that the flow behaviour strongly depends on the solution-to-binder (S/B) ratio, concentration of sodium hydroxide (NaOH), and sodium silicate-to-sodium hydroxide (SS/NaOH) ratio. Mortars with 0.4 S/B ratio were more consistent and afterwards adjusted with SP and more water to get the required flow[47]. Conversely, the mortars with S/B ratio of 0.5 was more flowable due to the higher volume of activator solution available for particle lubrication[45]. But later in this article, we will see that too much liquid also reduced early-age strength of these mixes. The reduction in flow observed at higher NaOH molarity may be associated with increased dissolution of aluminosilicate species and faster reaction kinetics reported in previous geopolymer studies[5]; [34]; [49]. However, since rheological parameters and setting characteristics were not directly measured in the present study, this interpretation is limited to qualitative comparison with existing literature[80]; [79]. As the NaOH concentration increases from 8M to 16M, the flow decreased due to improved dissolution of aluminosilicate precursors leading to rapid thickening of paste[92]. This is due to elevated concentrations of NaOH disrupting the, charge neutrality of solution enhancing the ionic activity of the OH^- group and consequently increasing the polymerisation and polycondensation activity[91]. This causes the paste to become denser and less flowable. As a result, it requires external amendments like superplasticizer addition to regain flowability. The SS/NaOH ratio also affected the flow behaviour, where increasing the SS/NaOH ratio from 0.1 to 2.5 reduced the mortar spread progressively[93]. Similar trends have been reported in previous studies where increased silicate modulus resulted in higher mixture cohesion and reduced flowability, which was attributed to increased gel formation and reduced free water content[94]. The mixes with SS/NaOH ratios below 0.5 showed relatively higher values which indicated good flow for the mortar. However, the workability reduced immensely at SS/NaOH of 1.5, due to which controlled dosing of superplasticiser and minimum addition of extra water was done [39]. The interaction of NaOH concentration and SS/NaOH ratio also contributed to flow behaviour, and this had a nonlinear effect on workability [95]. The influence of the SS/NaOH ratio was less prominent at notable NaOH molarities (either 8M or 12M) as mortars had good spread for all ratios tested. However, at higher molarities (14M and 16M), flowability drastically

declined beyond an SS/NaOH ratio of 1.5. This was the threshold beyond which excess silica content results in over-polymerization [96]. Hence, the paste becomes less fluid. High dosage of sodium silicate causes highly cohesive mixture which is beneficial in long-term strength development but unfavourable in fresh state workability [97]. The modifications made in this study ensured that mortars were within the prescribed flow limits, homogeneous with no segregation [98]. The summarized flow values presented in Table 3 and Table 4 clearly indicate the influence of activator composition and workability adjustment parameters on the fresh properties of geopolymer mortar, which subsequently influence strength development discussed in Section 4.4.

4.4. Compressive Strength Development in Geopolymer Mortars

The compressive strength of geopolymer mortars indicates the structural performance and durability of the mortar. As part of the study, strength development trends were evaluated using compressive strength tests at 3, 7 and 28 days under different activator and mix proportions. During mixing, limited adjustment using super plasticizer and/or small quantities of additional water was carried out only to achieve workable consistency necessary for proper casting of specimens [99]. The adjustments were maintained within a narrow range across all mixes and were not intended to modify the designed solution-to-binder ratio. The dosage of superplasticizer and additional water used for each mix is summarized in Table 3 and Table 4. Since the adjustments were minimal and consistently applied, their influence on compressive strength development is considered secondary compared to the dominant effects of activator composition and molarity. Nevertheless, this potential influence is acknowledged when interpreting strength variations among mixes [100].

In the present study, the H_2O/Na_2O ratio represents the mass ratio between the total water content present in the activating solution (including water from sodium silicate and sodium hydroxide solutions) and the equivalent sodium oxide (Na_2O) content contributed by the alkaline activator [69]. This parameter governs the effective alkalinity and availability of free water during geopolymerization. Lower H_2O/Na_2O ratios correspond to higher alkali concentration and increased dissolution of aluminosilicate species, whereas higher values indicate dilution of the activating medium [88]. The threshold ranges discussed in this study are therefore interpreted in relation to activator concentration and solution-to-binder ratio, ensuring consistency with the mix proportions presented in Tables 1 and 2.

The solution to binder(S/B) ratio, NaOH molarity and SS/NaOH ratio affects the rate of strength gain and the final compressive strength significantly and are represented in Fig.4 and Fig. 5. The compressive strength trends observed in Fig. 4 and Fig. 5 indicate that mixes with S/B = 0.4 consistently achieved higher strength compared to S/B = 0.5 across all NaOH molarities and SS/NaOH ratios[101]. At 28 days, the compressive strength ranged between approximately 6–50 MPa for S/B = 0.4 and 8–68 MPa for S/B = 0.5, with the maximum strength of 68 MPa recorded for mix 16GM1.5. Each reported strength value represents the average of n = 3 specimens, and the variation among specimens remained within acceptable experimental limits (±SD MPa). The higher strength obtained at lower S/B ratio is attributed to reduced free liquid content and formation of a denser geopolymer matrix, as clearly reflected by the strength trends shown in Fig. 4 and Fig. 5. Mortars that had an S/B ratio of 0.4 showed stronger strength values than those that had an S/B ratio of 0.5. This shows that an excessive liquid to binder ratio may dilute the geopolymer gel network, thereby weakening it [88]. As NaOH molarity increased the compressive strength also increased, with 68 MPa recorded at 28 days for 16M NaOH at SS/NaOH is 1.5 (16GM1.5), which was the maximum value observed. The concentration effect of NaOH on the strength development was most significant during early curing [63]. At 3 days the 8M and 12M NaOH mortars had rather low strengths in the range of 5 to 18 MPa depending on SS/NaOH ratio. However, by 7 days, strength was considerably higher, especially in mixes with 14M and 16M NaOH, which had strength values higher than 30 MPa in most cases. The quick strength development in mixes with high molarity can be related to the increase in the rate of dissolution of aluminosilicate precursors [102]. This results in faster gel formation and improved polymerization kinetics. Studies have also reported similar outcomes [63]. Higher NaOH molarity accelerates the formation of N-A-S-H gels and associated strength gain at early age [103]. However, it has been shown that strength can, however, start falling beyond an optimal concentration of 16M NaOH. Further increases in NaOH can cause high thermal energy release during its exothermic activation which causes microstructural inconsistencies [104].

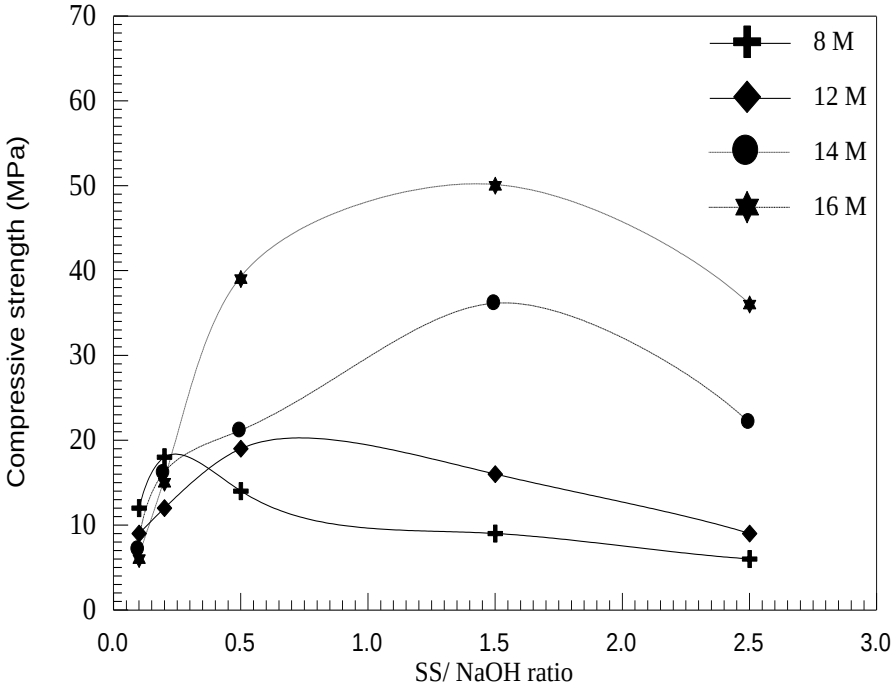

Figure 4. The 28 days compressive strength variation with SS/ NaOH ratio for S/B ratio of 0.4

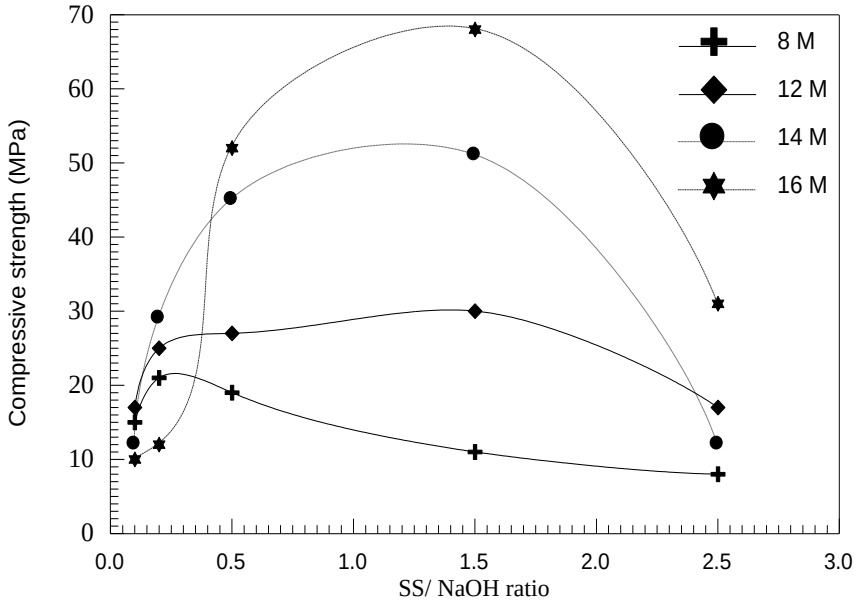

Figure 5. The 28 days compressive strength variation with SS/ NaOH ratio for S/B ratio of 0.5

Several previous studies have reported that the increase in NaOH molarity enhances compressive strength up to an optimum level due to improved dissolution of silica and alumina from fly ash particles and accelerated geopolymerization reactions [105]. For instance, fly ash–based geopolymer mortars incorporating nano-metakaolin showed significant strength improvement with increasing alkaline concentration owing to enhanced formation of aluminosilicate gels and reduced unreacted particles within the matrix. Similarly, studies on calcium-rich geopolymer systems have demonstrated that higher NaOH molarity promotes the formation of hybrid binding gels such as N–A–S–H and C–A–S–H, resulting in denser microstructures and improved compressive strength development at early ages [81].

The pronounced early-age strength gain observed in mixes with higher NaOH molarity is consistent with previous findings where increased alkalinity accelerated precursor dissolution and shortened the induction period of

geopolymerization. Research on fly ash–based geopolymer mortars has shown that higher alkali concentrations significantly enhance early strength development, although the rate of strength gain stabilizes at later ages once polymerization becomes diffusion controlled [106].

SS/NaOH ratio was also found important for the development of strength. The effective range was found between 1.0 and 1.5. Strength development was impeded due to the unavailability of significant or sufficient soluble silica at lower SS/NaOH ratios (0.1 and 0.2). Mixtures having SS/NaOH ratio of 1.5 produced maximum compressive strength and thereafter decline in strength was noticed. Strength decreases at SS/NaOH = 2.5 is due to a large amount of unreacted silicate species which did not polymerise leading to lower gel density [107]. The earlier findings of that ultimately at extremely high silicates, the system becomes supersaturated and chains formed are not effective, resulting in loss of mechanical strength [104].

The existence of an optimum SS/NaOH ratio observed in the present study is also consistent with earlier investigations. Increasing sodium silicate content improves the availability of soluble silica, promoting gel formation and strength enhancement up to an optimum level [72]. However, excessive silicate content increases mixture viscosity and reduces effective alkali mobility, thereby limiting further geopolymerization. Previous studies on geopolymer mortars cured under ambient conditions reported that increasing silicate modulus beyond an optimum value resulted in reduced compressive strength despite improved workability, indicating the existence of a balanced activator composition for maximum strength development [70].

In the present investigation, the reduction in strength beyond SS/NaOH = 1.5 was observed at higher NaOH molarities for both S/B ratios, as evident from Fig. 4 and Fig. 5, where the increase in silicate content did not translate into further strength gain [106]. Similar observations were reported in geopolymer systems where excessive silicate concentration resulted in incomplete reaction and increased pore connectivity due to excess free water associated with sodium silicate solutions [108]. Microstructural studies have shown that excessive silicate content may hinder the formation of a continuous geopolymer network, leading to reduced mechanical performance [84].

This shows that the required balance between Na_2O and SiO_2 should be maintained for better geopolymerization. The strength development effects of water content were also assessed and are largely represented through H_2O/Na_2O ratio [86]. A mortar with more S/B value will have a lower compressive strength if the H_2O/Na_2O excess. In combinations where the H_2O/Na_2O ratio was greater than 14, compressive strength values were substantially lower indicating that excess free water may hinder proper gel formation by increasing porosity. In contrast, H_2O/Na_2O in the range of 11–14 recorded the optimum strength values; thus, it can be assumed that the availability of water should be adequately controlled for maximum geopolymerization efficiency. The higher strength obtained for S/B = 0.4 compared to S/B = 0.5 is consistent with earlier findings that excessive liquid content increases pore volume and reduces matrix compactness. Studies on geopolymer mortars incorporating industrial by-products have demonstrated that lower liquid-to-binder ratios produce denser gel structures and improved interparticle bonding, resulting in higher compressive strength [101]. The results coincide with the findings, which indicate that the appropriate water/activator ratio minimizes defects and allows gel densification.Overall, the strength development trends observed in this study—namely the increase in strength with NaOH molarity up to an optimum level, the existence of an optimum SS/NaOH ratio around 1.5, and the reduction in strength at higher liquid contents—are consistent with previously reported geopolymer systems, confirming that compressive strength is governed by the balance between activator concentration, silica availability, and effective gel formation [92].

4.5. Factors Influencing Workability and Strength of Geopolymer Mortars

The workability and strength of geopolymer mortars are influenced by the interaction of factors such as the NaOH molarity, the SS/NaOH ratio, the water, and Na_2O/SiO_2 ratio. The dissolution rates of the fly ash precursor and the rate of polymerization, along with the overall microstructural development of the hardened geopolymer. While workability is important for ease of mixing, casting, and compaction of mortar, it is challenging to strike a balance between workability and compressive strength, since with increase in activator concentration, strength improves but flowability gets compromised [109]. This section describes the important parameters affecting the fresh and hardened properties of geopolymer mortars. A direct correlation between strength as well as workability and the NaOH concentration was found for all the mixes. As the NaOH concentration increased from 8M to 16M, a decrease in workability was noticed which necessitated the addition of superplasticizers and excess water to achieve a flow of 130 ± 10%. As the activator solution's viscosity is higher and rate of dissolution of fly ash is higher, it happens essentially

polycondensation takes place and due to which instant stiffening takes place[105]. Nevertheless, even though the workability dropped, it was noticed that the compressive strength increased, with the maximum value being 68 MPa at 28 days with 16M NaOH and SS/NaOH = 1.5. This trend agrees where higher leaching of Si^{4+} and Al^{3+} species from fly ash leads to denser and more homogeneous geopolymeric gels with an increase in NaOH concentration [100]. At NaOH molarity that is equal to or less than 8M, dissolution does not take place either, so the polymeric chains are weak and generate low compressive strength. Too much NaOH beyond 16M will not contribute to strength gain and will have higher chances of microcracking due to the fast and high exothermic reaction [93].

Table 3. Flow value and compressive strength of Mortars with Solution to binder ratio of 0.4

S.No	Superplasticizer (SP) (% of FA)	Molarity (M)	Extra Water (kg)	Flow Value (cm)	Mean Compressive strength (MPa)(n=3)			Standard Deviation for (28 days)
					3 Days	7 Days	28 Days	
1	0	8	0	128	9	9	12	1.6
2	0.3	8	0	126	18	20	22	1.8
3	0.8	8	0.012	130	11	14	16	1.2
4	1.2	8	0.031	129	9	10	11	1.25
5	1.4	8	0.041	128	5	5	6	1.2
6	0	12	0.011	127	7	8	9	1.65
7	0.7	12	0.022	129	8	10	12	1.4
8	1.2	12	0.03	126	14	16	19	1.5
9	1.7	12	0.045	131	11	14	16	1.75
10	2	12	0.06	130	5	7	9	1.45
11	0	14	0.017	129	4	6	7	1.2
12	1	14	0.026	128	12	14	16	1.65
13	1.4	14	0.039	129	16	18	21	1.25
14	1.6	14	0.051	127	32	35	36	0.85
15	2	14	0.075	126	17	21	22	1.2
16	0	16	0.034	128	5	6	6	1.3
17	1.5	16	0.041	129	11	12	15	1.6
18	1.7	16	0.058	130	31	35	39	1.4
19	2	16	0.077	131	47	49	50	1.5
20	2	16	0.081	130	33	34	36	1.4

Table 4 Flow value and compressive strength of Mortars with Solution to binder ratio of 0.5

S.No	Molarity (M)	Superplasticizer (SP) (% of FA)	Extra Water (kg)	Flow value (cm)	Mean Compressive Strength (MPa) (n=3)			Standard Deviation for (28 days)
					3 Days	7 Days	28 Days	
1	8	0	-	125	12	1.6	15	1.45
2	8	0.3	-	126	19	1.8	21	1.86
3	8	0.8	-	130	17	1.2	19	1.23
4	8	1.2	-	129	10	1.25	11	1.25
5	8	1.4	-	128	6	1.2	8	1.25
6	12	0	-	127	14	1.65	17	1.65
7	12	0.7	-	124	21	1.4	25	1.46
8	12	1.2	-	126	23	1.5	27	1.54
9	12	1.7	-	131	26	1.75	30	1.75
10	12	2	-	130	14	1.45	17	1.45
11	14	0	-	129	9	1.2	12	1.25
12	14	1	-	128	24	1.65	29	1.65
13	14	1.4	-	129	41	1.25	45	1.25
14	14	1.6	-	127	46	0.85	51	0.85
15	14	2	0.014	126	9	1.2	12	1.23
16	16	0	-	128	8	1.3	10	1.30
17	16	1.5	-	129	11	1.6	12	1.62
18	16	1.7	-	130	49	1.4	52	1.45
19	16	2	0.014	131	62	1.5	68	1.50
20	16	2	0.022	130	24	1.4	31	1.45

Furthermore, the workability and strength characteristics are examined for varying SS/NaOH ratios. Increasing the SS/NaOH from 0.1 to 2.5 affected flowability similar to what reported where sodium silicate concentration increased the total viscosity of the activator solution. This happens because of excess silica which promotes a high gel but at the same time also makes it cohesive[6]. However, even though workability decreased, the compressive strength increased with the rising ratio of SS/NaOH, reaching a maximum value at SS/NaOH = 1.5 after which strength decreased[29]. The drop after SS/NaOH = 1.5 is because of supersaturation, or too much sodium silicate which means there are extra silica species that do not effectively react to form the geopolymer. The results indicate that the NaOH molarity and SS/NaOH ratio should be optimized simultaneously, since neither parameter alone is sufficient to control workability and strength [110]. How much water you put in is another important factor affecting strength development, especially H_2O/Na_2O ratio. Additional water (1% - 8% by weight of fly ash) was necessary to maintain workability, especially for high molarity mixes which were limited by viscosity [13]. However, excessive water was detrimental to strength, as evidenced by mixes whose H_2O/Na_2O ratio was greater than 14, which reduced compressive strength. The highest strength was recorded at H_2O/Na_2O = 11 to 14. Here, the ambient moisture in the fly ash enables polymerization, which doesn't lead to excessive porosity [111]. As water content was increased further, beyond a certain critical level, the packing density of the gel would be reduced, which weakens the hardened structure (Van Jaarsveld et al. 2002). The comparative analysis of the two mix proportions adopted in the study (i.e., S/B = 0.4 and 0.5) indicates higher strength values for mortars with S/B = 0.4.

This corroborates the hypothesis that an excessive activator-to-binder ratio could further dilute the reaction product, compromising the bond among the matrix components [98]. The mechanical performance of the mortars was furthermore controlled by the Na2O/SiO2 ratio, as the maximum compressive strength was achieved when the Na2O/SiO2 ratio was 0.15 and 0.17. The ideal supersaturation scenario is attained at this range when the concentration of Al^{3+} and Si^{4+} species are high enough to polymerize but low enough to not phase segregate [112]. As the inclusion of Na_2O increased further than ideal levels, compressive strength started to decline further indicating that an overlap of the polymeric network formation took place. The XRD analysis depicts hydroxysodalite zeolite phases which confirm that geopolymerization was most effective in this Na_2O/SiO_2 range [113].

4.6. Effect of Water Content on Strength Development

Water is important to geopolymerization where it affects the workability when fresh and strength while hardened. The role of water in geopolymerization is quite different compared to Portland cement systems. In the latter, water mainly induces hydration whereas in the geopolymer mortar systems water acts a reaction medium that solubilizes aluminosilicate precursors and further condenses the aluminate and silicate polymer chains [93]. But too much water will dilute the geopolymer matrix and lead to an increase in porosity and the mechanical performance will drop [102]. The compressive strength of geopolymer mortars made with NaOH and sodium silicate was evaluated at different ratios of H_2O/Na_2O. In the present study, the H_2O/Na_2O ratio is defined on a mass basis as the ratio between the total water content present in the activating solution and the equivalent sodium oxide (Na_2O) content contributed by the alkaline activators. The total water content includes water present in the sodium silicate solution, water used for dissolving NaOH pellets, and any additional water added during mixing to achieve workable consistency. This definition was adopted to represent the effective dilution level of the activating solution and to maintain consistency across mixes with different activator compositions [114]. In the study, four different molarities of NaOH (8M to 16M) and four different SS/NaOH ratios (0.1 to 2.5) were used. According to the results, plasticity is governed by H_2O/Na_2O, beyond which strength fails. The variations in the compressive strength to H_2ONa_2O ratio is shown in Fig.6, Fig. 7 and Fig. 8 respectively. These figures show how strength varies with different NaOH concentrations at 3, 7, and 28 days. The results indicate that the best strength values were obtained when the H_2O/Na_2O was between 11 and 14. Mortars with S/B = 0.4 performed better than mortars with S/B = 0.5, which suggests that an excess of liquid causes dilution of the geopolymer gel network [43]. When the H_2O/Na_2O climbed above 14, the strength values dropped down because there were extra capillary pores that formed in the matrix. Similar result obtained where the water beyond the required limit causes microstructural defect leading to less densely packed geopolymer gel. When the ratio was below 11, workability was seriously

affected leading to mixes which were difficult to compact and were inhomogeneous [37].

During specimen preparation, limited adjustments using superplasticiser and/or small quantities of additional water were made only to achieve workable consistency required for casting. These adjustments were maintained within a narrow range across all mixes and were not intended to modify the designed solution-to-binder ratio. The dosage variations were minimal and applied consistently, thereby minimizing their influence on compressive strength trends. Consequently, the observed strength variations are primarily attributed to changes in H_2O/Na_2O ratio rather than workability adjustments. Nevertheless, this potential influence is acknowledged when interpreting the effect of water content on strength development [115].

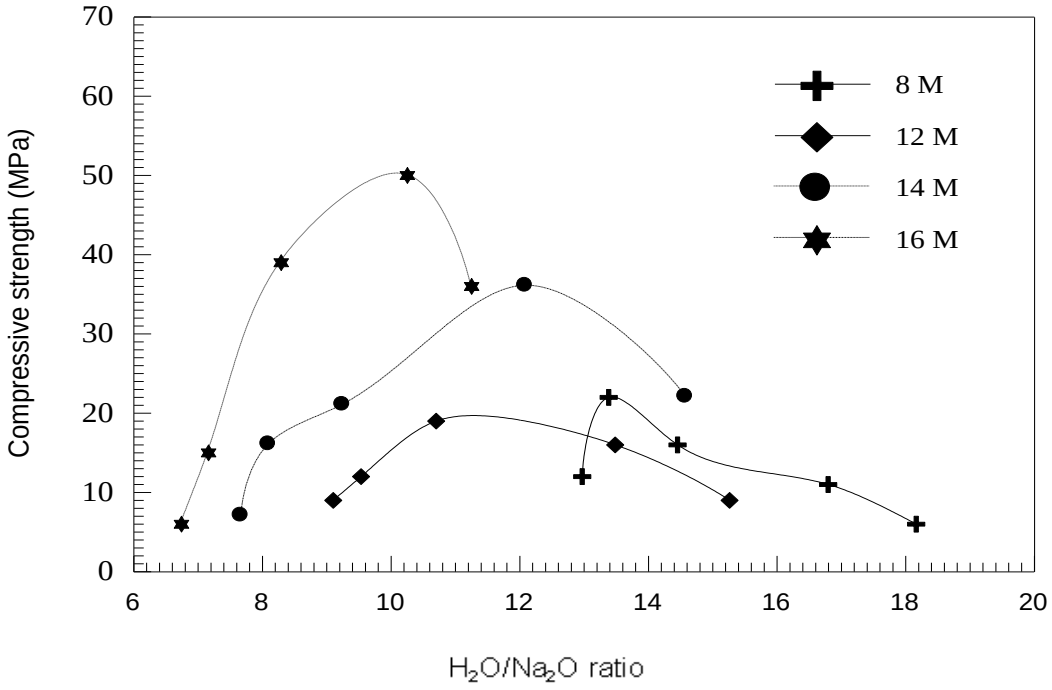

Figure 6. Variation of compressive strength with H_2O to Na_2O ratio for solution/b of 0.4

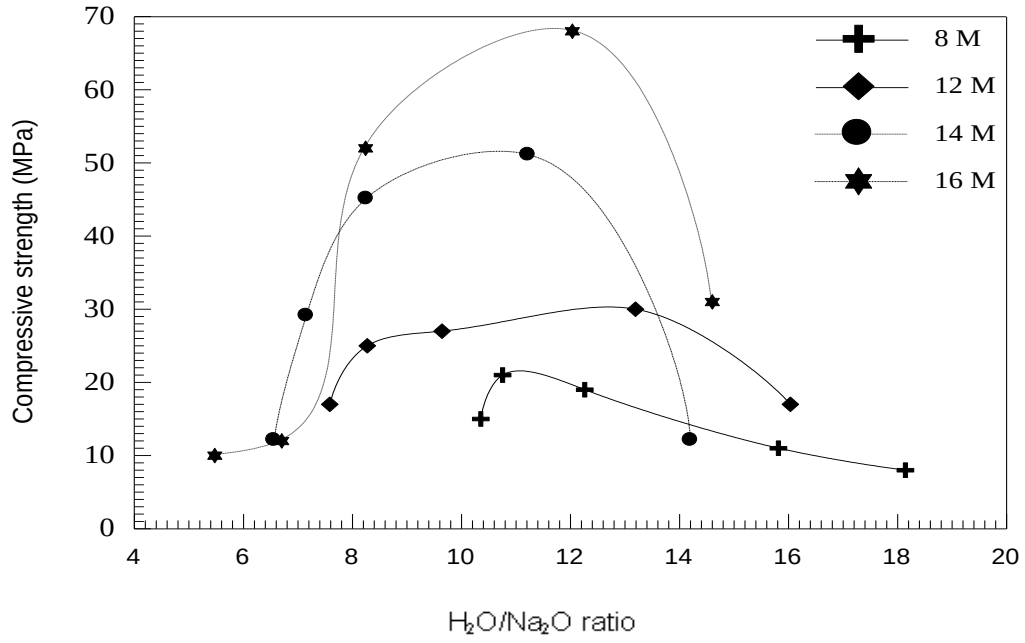

Figure 7. Variation of compressive strength with H_2O to Na_2O ratio for solution/b of 0.5

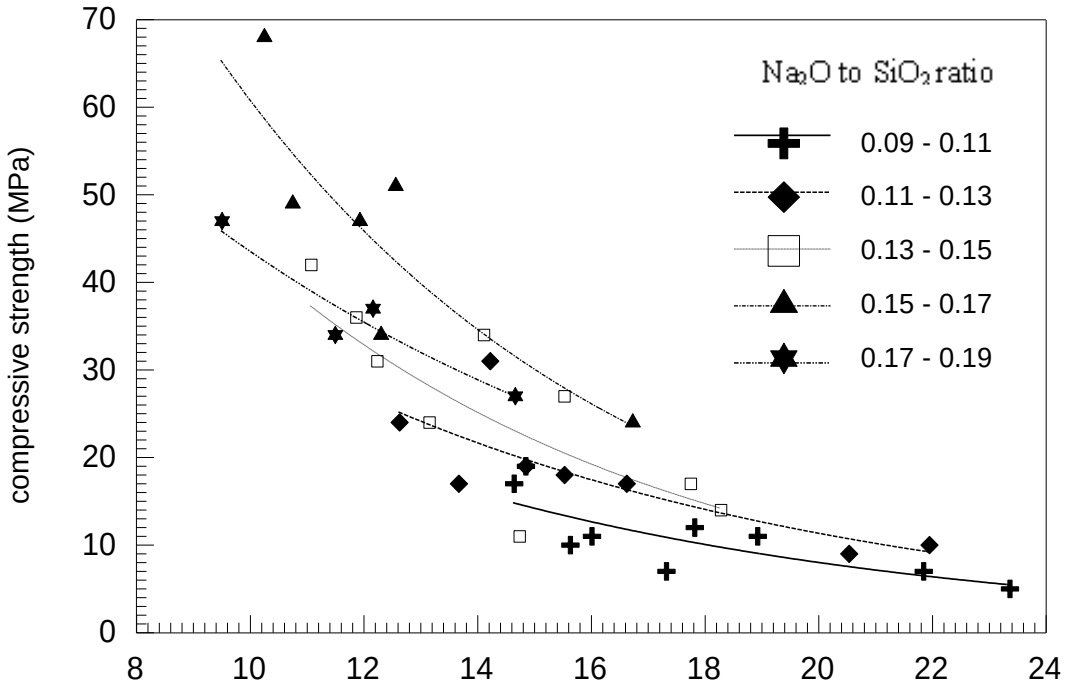

Figure 8. Compressive strength variation of mortar with various H_2O to Na_2O ratios and Na_2O to SiO_2 ratios

The Na_2O/SiO_2 ratio is also important for determining the alkali activation and the availability of silicates which subsequently impacts strength development. The experimental results indicate that strength peaked when Na_2O/SiO_2 ranged from 0.15 to 0.17, after which reductions were observed. This means that Na_2O/SiO_2< 0.15, the sodium oxide is not sufficient enough to activate the fly ash and the formation of geopolymer gel is incomplete. Meanwhile, at higher Na_2O/SiO_2 ratios (> 0.17), due to oversaturation of alkalis the polymerization process is hampered, leading to weaker networks with lower compressive strength[41]. The presence of hydroxysodalite peaks in the XRD patterns suggests the formation of crystalline aluminosilicate phases under higher alkali conditions. However, since quantitative phase analysis of amorphous content was not performed, the relationship between hydroxysodalite formation and maximum geopolymerization is interpreted qualitatively. The strength improvement is therefore attributed primarily to the overall balance between activator composition and gel formation rather than to a single crystalline phase[22]. We studied the extra water and SS/NaOH ratio together. It was found that a high SS/NaOH ratio required addition of extra water for maintaining workability. When the SS/NaOH has crossed 1.5, the workability was reduced despite the added extra water and compressive strength[68]. To enhance workability, one has to compromise on strength due to extra water, hence, must be optimally used in high early-age strength applications. According to the results, the effect of additional water is more strong in case of higher molarity NaOH mixes (14M and 16M), where gel formation is already taking place rapidly. It is clear from the results that the water content must be controlled to provide good workability and strength[63]. The ideal ranges for an optimized geopolymer matrix development were found to be H_2O/Na_2O 11–14 and Na_2O/SiO_2 0.15–0.17. In the present study, the Na_2O/SiO_2 ratio was calculated on a molar basis, considering the total Na_2O and SiO_2 contributed by both sodium hydroxide and sodium silicate solutions in the activating system. The Na_2O content from NaOH and sodium silicate and the soluble SiO_2 from sodium silicate were included in the calculation to represent the overall alkalinity and silica availability governing geopolymerization[3]. Any departure from these values led to microstructural instability, lower polymerization efficiency, and reduced mechanical strength. According to this statement, controlled water addition strategies must be implemented such that the geopolymer mortars achieve a balance between having sufficient fluidity during mixing and placement and having the required densification for high mechanical performance[41].

Previous studies have similarly reported that compressive strength in fly ash–based geopolymer systems is strongly governed by the balance between alkali concentration and available soluble

silica, where insufficient alkali limits dissolution of aluminosilicate precursors, while excessive alkali concentration leads to incomplete polymer network formation and increased pore connectivity. Studies on fly ash and slag-based geopolymer mortars have shown that optimum Na_2O/SiO_2 ratios promote the formation of a continuous aluminosilicate gel network, whereas excessive alkali content may result in the formation of secondary crystalline phases and reduced mechanical performance[48]; [116].

For mixes with higher SS/NaOH ratios, limited additional water and superplasticiser were introduced to maintain workable consistency during casting. The quantities added were maintained within a narrow range and are summarized in Table X. These adjustments were applied only to achieve comparable workability and were not intended to modify the designed activator composition. While additional water may influence porosity and compressive strength, the observed strength trends remained consistent with changes in Na_2O/SiO_2 and H_2O/Na_2O ratios, indicating that activator chemistry remained the dominant factor governing strength development[117].

4.7. Mathematical analysis

The water-to-sodium oxide ratio and 28-day compressive strength of geopolymer mortar were investigated for two solution-to-binder ratios: 0.4 and 0.5. Higher-order polynomial models were developed to help understand the trends of strength development, which aid in finding a non-linear relationship. According to the results, compressive strength is very sensitive to the water-to-Na_2O ratio. An optimal range exists beyond which compressive strength reduces due to excess water content leading to dilution effects and greater porosity[2].

The empirical equation that expresses compressive strength as a function of mix parameters is presented below in Equation 1.

$$\sigma_c = f\left(M, \frac{SS}{NaOH}, NaOH, \frac{H_2O}{Na_2O}, \frac{Na_2O}{SiO_2}\right) \quad (1)$$

A possible functional form can be derived using nonlinear least-squares approximation and it is as represented in Equation 2

$$\sigma_c = A \times \left(\frac{SS}{NaOH}\right)^m + B \times M^n + \\ + C \times \left(\frac{Na_2O}{SiO_2}\right)^p + D \times e^{\left(\frac{-H_2O}{Na_2O}\right)} \quad (2)$$

where, A, B, C, D, m, n, p are empirical constants to be determined using curve fitting from the dataset

By the polynomial regression model for the mortar mix of solution-to-binder ratio 0.4, multiple critical points were identified. The strength of the mortar mix first increased with water-to-Na_2O ratio and then dropped. This shows that there is an adequate balance between the water required for geopolymerization and retaining the integrity of the matrix. For the mortar mix with a solution-to-binder ratio of 0.5, a pattern similar to that for the 0.4 ratio was noted, yet the coefficients of the polynomial model suggested a sharper decline in strength at increasingly higher water-to-Na_2O ratios. This sharper decline could be owing to excessive pore formation which impacted the densification of the matrix[52].

Based on the tabulated results from Table 3 and Table 4, the predictive equations are derived and are presented in Equation 3 and Equation 4 for the two binder ratios.

For Solution/Binder Ratio = 0.4,

$$\sigma_c = -518.52 + \left(\frac{-18.15 \times SS}{NaOH}\right) + 9.10 \times M + 78.97 \times \left(\frac{Na_2O}{SiO_2}\right) + 10.17 \times \left(\frac{H_2O}{Na_2O}\right) \quad (3)$$

Here, the $\left(\frac{H_2O}{Na_2O}\right)$ ratio and NaOH Molarity contribute positively to strength, whereas, the $\left(\frac{SS}{NaOH}\right)$ ratio has a negative impact on strength. But on the contrary, $\left(\frac{Na_2O}{SiO_2}\right)$ ratio shows a strong positive correlation.

Similarly, For Solution/Binder Ratio = 0.5

$$\sigma_c = -87.88 + \left(\frac{-37.41 \times SS}{NaOH}\right) + 8.11 \times M + (-348.7) \times \left(\frac{Na_2O}{SiO_2}\right) + 5.18 \times \left(\frac{H_2O}{Na_2O}\right) \quad (4)$$

Here, the SP Content has a positive influence on compressive strength, whereas, both $\left(\frac{SS}{NaOH}\right)$ and $\left(\frac{Na_2O}{SiO_2}\right)$ ratios negatively affect strength. But just as expected, $\left(\frac{H_2O}{Na_2O}\right)$ratio has a small positive influence. It is to be noted that NaOH Molarity positively influences compressive strength.

The general form of the Higher-Order Polynomial Model is given as below in equation 5.

$$\sigma_c = \beta_0 + \sum_{i=1}^{n} \beta_i X_i + \sum_{j=1}^{n} \beta_j X_j^2 + \sum_{k=1}^{n} \beta_k X_k^3 + \varepsilon \quad (5)$$

For S/B =0.4 and S/B = 0.5, the same higher order polynomial model is derived as in equation 6.

$$\sigma_c = \beta_0 + \beta_1\left(\frac{SS}{NaOH}\right) + \beta_2(NaOH_M) + \beta_3\left(\frac{H_2O}{Na_2O}\right) + \beta_4\left(\frac{Na_2O}{SiO_2}\right) + \beta_5\left(\frac{SS}{NaOH}\right)^2 + \beta_6(NaOH_M)^2 + \\ +\beta_7\left(\frac{H_2O}{Na_2O}\right)^2 + \beta_8\left(\frac{Na_2O}{SiO_2}\right)^2 + \cdots + \varepsilon \quad (6)$$

Based on the analysis, following equations – 7, 8 are developed as the higher order polynomial equations towards the relationship between H_2O/Na_2O ratio and Compressive Strength (MPa) at 28 Days.

For, Solution/Binder Ratio = 0.4,

$$\sigma_c = 1.0971 \times 10^{-2}x^4 - 0.4485x^3 + 5.6343x^2 - 19.5683x - 2.1185 \quad (7)$$

For, Solution/Binder Ratio = 0.5,

$$\sigma_c = 6.2628 \times 10^{-3}x^4 - 0.2316x^3 + 2.0264x^2 + 5.2474x - 49.8802 \quad (8)$$

Here, x represents the $\left(\frac{H_2O}{Na_2O}\right)$ ratio.

The fitted polynomial models show the interaction of geopolymer mix design parameters with strength evolution more comprehensively. They are presented in Fig.9 and Fig.10. The polynomial regression graphics for S/B ratios of 0.4 and 0.5 show a non-linear relationship between the water-to-Na_2O ratio and 28-day compressive strength. In both the cases, it is noticed that initially strength goes on increasing, till optimum range is achieved, but on increased water-to-Na_2O ratio, strength again starts falling[88].

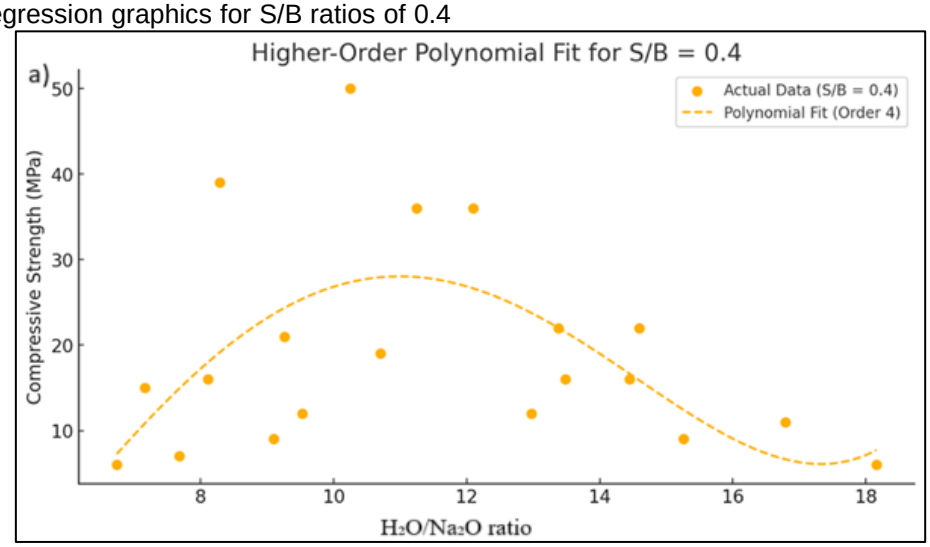

Fig. 9 Higher Order Polynomial Fit for S/B ratio of 0.4

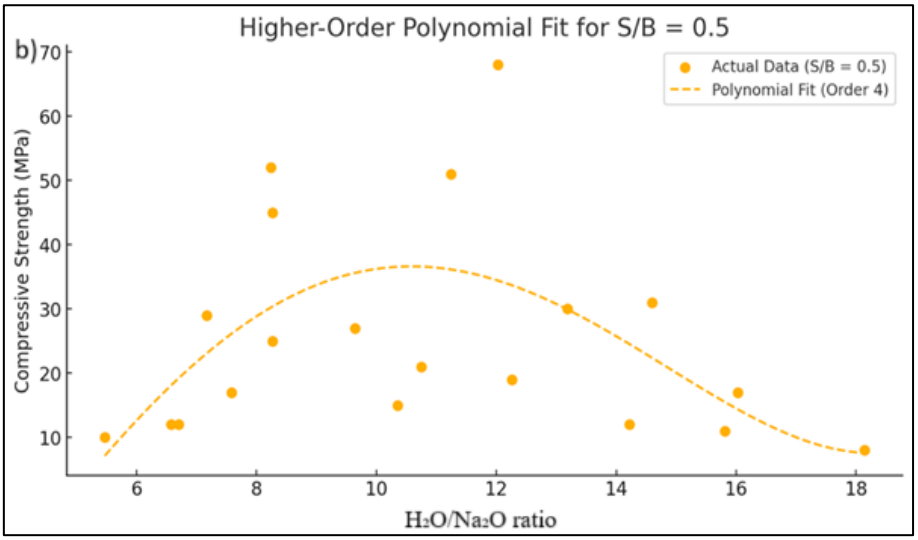

Fig. 10 Higher Order Polynomial Fit for S/B ratio of 0.5

The S/B = 0.4 mixture has a wide strength plateau which indicates greater stability before the onset of strength reduction. Thus, the compressive strength of S/B = 0.5 mixture displays a steep drop in value at large water contents due to excessive porosity formation. The additional terms in the polynomial models indicate it is not a simple input-output relationship[118]. One can expect properties to be influenced by hydration, geopolymerization kinetics and microstructural densification. The equations derived enable an estimation of compressive strength based on mix design parameters to be made for geopolymer mortars.

4.8. Strength Evolution Model (Differential Equation Approach)

The compressive strength evolution of geopolymer mortars is a time-dependent process. Geopolymerization process involving dissolution, gel formation and hardening. A differential equation can be used to mathematically describe the evolution of time-dependent compressive strength of geopolymer mortars. This formulation factors in the dependence of strength gain on time, the presence of reactive species and curing conditions[116].

A first-order strength evolution model assumes that the rate of strength gain is proportional to the remaining potential strength development. Using our 3, 7, and 28-day compressive strength values, we can derive a strength evolution equation based on a differential formulation and is expressed in equation 9.

$$\frac{d\sigma_c}{dt} = k \times (\sigma_{max} - \sigma_c) \qquad (9)$$

where k = rate constant, σ_{max}= ultimate compressive strength (value at 28 days) and t = curing time (in days).

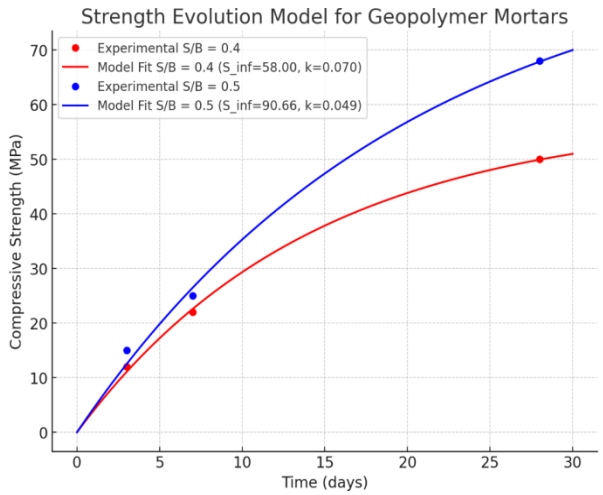

Fig. 11 Variation of Compressive strength through Strength Evaluation model fit

The key parameters showed that, S/B = 0.4; σmax =58.00 MPa and k = 0.0705 day^{-1} for the compressive strength of geopolymer mortar. This suggests that the strength developed rapidly at first but became constant as it approached the peak (Fig. 11). On the other hand, the obtained values for the S/B = 0.5 mixture produced a high ultimate compressive strength of 90.66 MPa but a lower rate constant of 0.0493 day−1. A slower rate of strength gain is shown in this case compared to the S/B = 0.4 mixture but greater final strength. The trend shows that as the solution-to-binder (S/B) ratio increases, the long-term strength improves but strength gain rate is slightly reduced. The early-age strength (3-7 days) of the S/B = 0.4 mix is lower than that of the S/B = 0.5 mix, reaffirming that the activator concentration has an impact on geopolymerization[115]. Despite the slower growth rate for the S/B = 0.5 mix, this could indicate a more extended reaction period that may be advantageous for long-term structural stability.

4. CONCLUSIONS

The present study systematically investigated the influence of alkali activator composition, including NaOH molarity, SS/NaOH ratio, solution-to-binder ratio, and water content, on the workability and compressive strength development of fly ash–based geopolymer mortars. Based on the experimental results and microstructural analysis, the following conclusions are drawn:

- Increasing NaOH molarity from 8M to 16M significantly enhanced compressive strength due to improved dissolution of aluminosilicate precursors and accelerated geopolymerization. The highest 28-day compressive strength of 68 MPa was achieved for the mix containing 16M NaOH with SS/NaOH = 1.5.
- The SS/NaOH ratio strongly influenced strength development. Compressive strength increased with SS/NaOH ratio up to an optimum value of 1.5, beyond which a reduction in strength was observed at SS/NaOH = 2.5 for both solution-to-binder ratios. This indicates that excessive silicate content does not contribute to further strength gain and may adversely affect polymer network formation.
- The H_2O/Na_2O ratio was found to govern both workability and strength development. In this study, the H_2O/Na_2O ratio was calculated on a mass basis considering the total water present in the activating system, including water from sodium silicate solution, NaOH solution, and any additional mixing water. An optimum range of H_2O/Na_2O between 11 and 14 provided the best balance between workability and compressive strength, while higher values

resulted in dilution of the activator and reduced mechanical performance.

- The Na_2O/SiO_2 ratio played a significant role in controlling geopolymer matrix formation. Optimum strength development was observed within the Na_2O/SiO_2 range of 0.15–0.17, while deviations from this range resulted in reduced strength, likely due to insufficient activation at lower ratios or excessive alkali concentration at higher ratios.
- X-ray diffraction analysis indicated the presence of zeolite-type aluminosilicate phases, including hydroxysodalite, suggesting structural reorganization of the geopolymer matrix with increasing activator concentration. However, since quantitative amorphous phase analysis was not performed, the relationship between crystalline phase formation and degree of geopolymerization is interpreted qualitatively.
- The influence of activator composition on compressive strength development was further represented using higher-order polynomial relationships and differential strength growth models, indicating non-linear strength progression with curing time and supporting the identification of optimum activator proportions.

Overall, the study demonstrates that careful control of activator composition and water content enables the production of high-strength geopolymer mortars with improved mechanical performance, highlighting the potential of fly ash–based geopolymer binders for high-performance and sustainable construction applications.

5. REFERENCE

[1] L. Yan, B. Kasal, L. Huang (2016). A review of recent research on the use of cellulosic fibres, their fibre fabric reinforced cementitious, geopolymer and polymer composites in civil engineering, Compos. Part B Eng., 92, 94-132, doi:10.1016/j.compositesb.2016.02.002.

[2] G.P. Lignola, V. Prota, F. Ceroni, E. Cosenza (2017). Performance assessment of basalt FRCM for retrofit applications on masonry, Compos. Part B Eng., 128, 1-18, doi:10.1016/j.compositesb.2017.05.003.

[3] B. Lee, G. Kim, R. Kim, B. Cho, S. Lee, C. Chon (2017). Strength development properties of geopolymer paste and mortar with respect to amorphous Si/Al ratio of fly ash, Constr. Build.Mater., 151, 512-519, doi:10.1016/j.conbuildmat.2017.06.078.

[4] S. Rocha, F. Pacheco-Torgal, Z.M. Zhang, J. Castro-Gomes, L.F. Ramos (2018). Metakaolin-based geopolymer mortars with different alkaline activators, Constr. Build.Mater., 178, 453-461, doi:10.1016/j.conbuildmat.2018.05.172.

[5] M.N.S. Hadi, M. Al-Azzawi, T. Yu (2018). Effects of fly ash characteristics and alkaline activator components on compressive strength of fly ash-based geopolymer mortar, Constr. Build. Mater., 175, 41-54, doi:10.1016/j.conbuildmat.2018.04.092.

[6] H.E. Elyamany, A.M. Elmoaty, M.A. Elmoaty, A.M. Elshaboury (2018). Magnesium sulfate resistance of geopolymer mortar, Constr. Build.Mater., 184, 111-127, doi:10.1016/j.conbuildmat.2018.06.212.

[7] J.H. Zhuang, H.Y. Zhang, H. Xu (2017). Resistance of geopolymer mortar to acid and chloride attacks, Procedia Eng., 210, 126-131, doi:10.1016/j.proeng.2017.11.057.

[8] N.A. Ulloa, H. Baykara, M.H. Cornejo, A. Rigail, C. Paredes, J.L. Gutierrez (2018). Application-oriented mix design optimization and characterization of zeolite-based geopolymer mortars, Constr. Build.Mater., 174, 138-149, doi:10.1016/j.conbuildmat.2018.04.101.

[9] S. Kumer, S. Al-Deen, M. Ashraf, W. Hutchison (2020). Resistance of fly ash-based geopolymer mortar to both chemicals and high thermal cycles simultaneously, Constr. Build. Mater., 239, 117886, doi:10.1016/j.conbuildmat.2019.117886.

[10] N.U. Kockal, T. Ozturan (2011). Durability of lightweight concretes with lightweight fly ash aggregates, Constr. Build. Mater., 25, 1430-1438, doi:10.1016/j.conbuildmat.2010.09.022.

[11] F. Ameri, P. Shoaei, S. Alireza, B. Behforouz (2019). Geopolymers vs. alkali-activated materials (AAMs): A comparative study on durability, microstructure, and resistance to elevated temperatures of lightweight mortars, Constr. Build. Mater., 222, 49-63, doi:10.1016/j.conbuildmat.2019.06.079.

[12] P. Shoaei, H. Reza, F. Mirlohi, S. Narimani, F. Ameri (2019). Waste ceramic powder-based geopolymer mortars: Effect of curing temperature and alkaline solution-to-binder ratio, Constr. Build. Mater., 227, 116686, doi:10.1016/j.conbuildmat.2019.116686.

[13] M. Vafaei, A. Allahverdi, P. Dong, N. Bassim (2018). Acid attack on geopolymer cement mortar based on waste-glass powder and calcium aluminate cement at mild concentration, Constr. Build. Mater., 193, 363-372, doi:10.1016/j.conbuildmat.2018.10.203.

[14] A. Gholampour, V.D. Ho, T. Ozbakkaloglu (2019). Ambient-cured geopolymer mortars prepared with waste-based sands: Mechanical and durability-related properties and microstructure, Compos. Part B Eng., 160, 519-534, doi:10.1016/j.compositesb.2018.12.057.

[15] S. Jin, Y. Ji, C. Lu, H. Wei (2026). Viability of fiber-reinforced geopolymer mortar as a protective layer for coal gangue concrete piles in cold regions: Balancing materials, applications, and sustainability, Compos. Part B Eng., 312, 113336, doi:10.1016/j.compositesb.2025.113336.

[16] M. Kaya, M. Junaid, S. Minhaj, S. Kazmi, O. Gencel (2026).Valorization of tile waste in geopolymer mortars: A sustainable approach using marble powder, fly ash, and silica fume, Powder Technol., 469, 121866, doi:10.1016/j.powtec.2025.121866.

[17] A. Sharma, P. Singh, K. Kapoor (2022). Utilization of recycled fine powder as an activator in fly ash-based geopolymer mortar, Constr. Build.Mater., 323, 126581, doi:10.1016/j.conbuildmat.2022.126581.

[18] S.J. Chithambaram, S. Kumar, M.M. Prasad (2020). Thermo-mechanical characteristics of geopolymer mortar, Constr. Build. Mater., 213, 100-108, doi:10.1016/j.conbuildmat.2019.04.051.

[19] F. Sahin, M. Uysal, O. Canpolat, T. Cosgun, H. Dehghanpour (2021). The effect of polyvinyl fibers on metakaolin-based geopolymer mortars with different aggregate filling, Constr. Build.Mater., 300, 124257, doi:10.1016/j.conbuildmat.2021.124257.

[20] Y. Wang, K. Peng, Y. Alrefaei, J. Dai (2021). The bond between geopolymer repair mortars and OPC concrete substrate: Strength and microscopic interactions, Cem. Concr.Compos., 119, 103991, doi:10.1016/j.cemconcomp.2021.103991.

[21] J.C. Kuri, P.K. Sarker, F. Uddin, A. Shaikh (2021). Sulphuric acid resistance of ground ferronickel slag blended fly ash geopolymer mortar, Constr. Build. Mater., 313, 125505, doi:10.1016/j.conbuildmat.2021.125505.

[22] J. Kwasny, T.A. Aiken, M.N. Soutsos, J.A. McIntosh, D.J. Cleland (2018). Sulfate and acid resistance of lithomarge-based geopolymer mortars, Constr. Build. Mater., 166, 537-553, doi:10.1016/j.conbuildmat.2018.01.129.

[23] A. Akbar, F. Farooq, M. Shafique, F. Aslam, R. Alyousef (2021). Sugarcane bagasse ash-based engineered geopolymer mortar incorporating propylene fibers, J. Build.Eng., 33, 101492, doi:10.1016/j.jobe.2020.101492.

[24] H. Rashidian-Dezfouli, P. Rao (2021). Study on the effect of selected parameters on the alkali-silica reaction of aggregate in ground glass fiber and fly ash-based geopolymer mortars, Constr. Build. Mater., 271, 121549, doi:10.1016/j.conbuildmat.2020.121549.

[25] M. Hoy, S. Thandar, S. Horpibulsuk (2025). Strength and microstructural evaluation of sustainable geopolymer mortars using calcium carbonate sludge and fly ash as precursors, Case Stud. Constr. Mater., 23, e05189, doi:10.1016/j.cscm.2025.e05189.

[26] K. Wang, P. Zhang, J. Guo, Z. Gao (2021). Single and synergistic enhancement on durability of geopolymer mortar by polyvinyl alcohol fiber, J. Mater.Res. Technol., 15, 1801-1814, doi:10.1016/j.jmrt.2021.09.036.

[27] H.E. Elyamany, A.M. Elmoaty, M.A. Elmoaty, A.M. Elshaboury (2018). Setting time and 7-day strength of geopolymer mortar with various binders, Constr. Build.Mater., 187, 974-983, doi:10.1016/j.conbuildmat.2018.08.025.

[28] J. Wang, L. Han, Z. Liu, D. Wang (2020). Setting controlling of lithium slag-based geopolymer by activator and sodium tetraborate as a retarder and its effects on mortar properties, Cem. Concr. Compos., 110, 103598, doi:10.1016/j.cemconcomp.2020.103598.

[29] H. Ilcan, O. Sahin, A. Kul, G. Yildirim, M. Sahmaran (2022). Rheological properties and compressive strength of construction and demolition waste-based geopolymer mortars for 3D printing, Constr. Build.Mater., 328, 127114, doi:10.1016/j.conbuildmat.2022.127114.

[30] Y. Sun, X. Wang, Y. Cao, Z. Chen, J. Fan, D. Liu (2025). Retardation behavior and mechanism of organic retarders on geopolymers at high temperatures and their effects on mortar properties, Constr. Build.Mater., 493, 143148, doi:10.1016/j.conbuildmat.2025.143148.

[31] X. Shi, C. Zhang, X. Wang, T. Zhang, Q. Wang (2022). Response surface methodology for multi-objective optimization of fly ash-GGBS based geopolymer mortar, Constr. Build. Mater., 315, 125644, doi:10.1016/j.conbuildmat.2021.125644.

[32] M. Vafaei, A. Allahverdi, P. Dong, N. Bassim, M. Mahinroosta (2021).Resistance of red clay brick waste/phosphorus slag-based geopolymer mortar to acid solutions of mild concentration, J. Build.Eng., 34, 102066, doi:10.1016/j.jobe.2020.102066.

[33] X. Guo, G. Xiong (2021). Resistance of fiber-reinforced fly ash-steel slag based geopolymermortar to sulfate attack and drying-wetting cycles, Constr. Build. Mater., 269, 121326, doi:10.1016/j.conbuildmat.2020.121326.

[34] W. Long, X. Zhang, J. Xie, S. Kou, Q. Luo, J. Wei (2022). Recycling of waste cathode ray tube glass through fly ash-slag geopolymer mortar, Constr. Build.Mater., 322, 126454, doi:10.1016/j.conbuildmat.2022.126454.

[35] R. Kunthawatwong, L. Sylisomchanh, S. Pangdaeng, A. Wongsa (2022).Recycled non-biodegradable polyethylene terephthalate waste as fine aggregate in fly ash geopolymer and cement mortars, Constr. Build.Mater., 328, 127084, doi:10.1016/j.conbuildmat.2022.127084.

[36] U. Durak, U. Bayram (2025). Recycled concrete aggregates in geopolymer mortars: Performance and environmental assessment, Constr. Build. Mater., 505, 144696, doi:10.1016/j.conbuildmat.2025.144696.

[37] A. Albidah, A. Abadel, F. Alrshoudi, A. Altheeb, H. Abbas, Y. Al-Salloum (2020). Bond strength between concrete substrate and metakaolin geopolymer repair mortars at ambient and elevated temperatures, J. Mater. Res. Technol., 9, 10732-10745, doi:10.1016/j.jmrt.2020.07.092.

[38] A. Wongsa, R. Kunthawatwong, S. Naenudon, V. Sata (2020). Natural fiber reinforced high calcium fly ash geopolymer mortar, Constr. Build. Mater., 241, 118143, doi:10.1016/j.conbuildmat.2020.118143.

[39] J. Sai, D. Neeraja (2018). Properties of class F fly ash based geopolymer mortar produced with alkaline water, J. Build. Eng., 19, 42-48, doi:10.1016/j.jobe.2018.04.031.

[40] C. Suksiripattanapong, K. Krosoongnern (2020). Properties of cellular lightweight high-calcium bottom ash-Portland cement geopolymer mortar,

Case Stud. Constr. Mater., 12, e00337, doi:10.1016/j.cscm.2020.e00337.

[41] O.A. Abdulkareem, M. Ramli, J.C. Matthews (2019). Production of geopolymer mortar system containing high calcium biomass wood ash as a partial substitution to fly ash: An early age evaluation, Compos. Part B Eng., 174, 106941, doi:10.1016/j.compositesb.2019.106941.

[42] S. Jiang, X. Wang, K. Qi, X. Wan (2025). Preparation and performance of a fast-hardening red mud based geopolymer repair mortar complexed with FGD, J. Build. Eng., 108, 112980, doi:10.1016/j.jobe.2025.112980.

[43] T. Yang, H. Zhu, Z. Zhang (2017). Influence of fly ash on the pore structure and shrinkage characteristics of metakaolin-based geopolymer pastes and mortars, Constr. Build. Mater., 153, 284-293, doi:10.1016/j.conbuildmat.2017.05.067.

[44] Y. Wang, S. Jin, X. Wang, T. Zhu, Q. Wang (2025). Polyvinyl alcohol fiber reinforced electrolytic manganese slag based geopolymer mortar: Mechanical properties and microstructure, Constr. Build. Mater., 477, 141390, doi:10.1016/j.conbuildmat.2025.141390.

[45] G.A. Soares, B.P. Bezerra, J.G. Antoniazzi, M.D.M. Innocentini (2025). Physico-mechanical and thermal behavior of foamed mortars bonded with Portland cement or metakaolin-based geopolymer, J. Build. Eng., 111, 113644, doi:10.1016/j.jobe.2025.113644.

[46] Y. Wang, K. Takasu, Q. Zhao, K. Harada, Z. Liu, H. Suyama (2025). Performance optimization and carbon reduction potential of bamboo biochar fine aggregates for sustainable geopolymer mortars, Constr. Build. Mater., 497, 143905, doi:10.1016/j.conbuildmat.2025.143905.

[47] M.G. Khalil, F. Elgabbas, M.S. El-Feky, H. El-Shafie (2020). Performance of geopolymer mortar cured under ambient temperature, Constr. Build. Mater., 242, 118090, doi:10.1016/j.conbuildmat.2020.118090.

[48] P. Darvish, U.J. Alengaram, Y. Soon, S. Ibrahim, S. Yusoff (2020).Performance evaluation of palm oil clinker sand as replacement for conventional sand in geopolymer mortar, Constr. Build.Mater., 258, 120352, doi:10.1016/j.conbuildmat.2020.120352.

[49] A. Bhutta, M. Farooq, N. Banthia (2019). Performance characteristics of micro fiber-reinforced geopolymer mortars for repair, Constr. Build.Mater., 215, 605-612, doi:10.1016/j.conbuildmat.2019.04.210.

[50] Y. Wang, X. Liu, Z. Zhang, Y. Li (2025). Performance and strength mechanism of aeolian sand mortar solidified by coal gangue-slag geopolymers, Case Stud. Constr. Mater., 23, e05567, doi:10.1016/j.cscm.2025.e05567.

[51] A. El Abd, S.E. Kichanov, M. Taman, R.M. Nazarov (2020). Penetration of water into cracked geopolymer mortars by means of neutron radiography, Constr. Build. Mater., 256, 119471, doi:10.1016/j.conbuildmat.2020.119471.

[52] W. Ye, H. Kruppa, A. Vollpracht, Y. Tan (2025). Paste rheological behavior and mortar workability of siliceous fly ash geopolymer, Constr. Build. Mater., 486, 142050, doi:10.1016/j.conbuildmat.2025.142050.

[53] D. Wang, K. Zou, S. Zhu, L. Guo (2025). Optimization of mix proportions and mechanical properties of coal gangue-based multi-solid-waste geopolymer mortars, Case Stud. Constr. Mater., 23, e05134, doi:10.1016/j.cscm.2025.e05134.

[54] L. Yan, Y. Li, F. Gao, X. Wang, H. Xu, R. Hai (2025). Optimization of mix proportion design for expanded perlite geopolymer insulating mortar based on mixture design, Constr. Build. Mater., 491, 142641, doi:10.1016/j.conbuildmat.2025.142641.

[55] E. Luga, C. Duran (2018). Optimization of heat cured fly ash/slag blend geopolymer mortars designed by Combined Design method: Part 1, Constr. Build. Mater., 178, 393-404, doi:10.1016/j.conbuildmat.2018.05.140.

[56] H.M. Khater, M. Ghareib (2020). Optimization of geopolymer mortar incorporating heavy metals in producing dense hybrid composites, J. Build.Eng., 32, 101684, doi:10.1016/j.jobe.2020.101684.

[57] A. Hasnaoui, E. Ghorbel, G. Wardeh (2019). Optimization approach of granulated blast furnace slag and metakaolin based geopolymer mortars, Constr. Build. Mater., 198, 10-26, doi:10.1016/j.conbuildmat.2018.11.251.

[58] A. Wongsa, R. Kunthawatwong, S. Naenudon, V. Sata, P. Chindaprasirt (2020). Natural fiber reinforced high calcium fly ash geopolymer mortar, Constr. Build. Mater., 241, 118143, doi:10.1016/j.conbuildmat.2020.118143.

[59] M. Kaur, J. Singh, M. Kaur (2018). Microstructure and strength development of fly ash-based geopolymer mortar: Role of nano-metakaolin, Constr. Build. Mater., 190, 672-679, doi:10.1016/j.conbuildmat.2018.09.157.

[60] J.C. Kuri, S. Majhi, P.K. Sarker, A. Mukherjee (2021). Microstructural and non-destructive investigation of the effect of high temperature exposure on ground ferronickel slag blended fly ash geopolymer mortars, J. Build. Eng., 43, 103099, doi:10.1016/j.jobe.2021.103099.

[61] A. Naghizadeh, S.O. Ekolu (2019). Method for comprehensive mix design of fly ash geopolymer mortars, Constr. Build. Mater., 202, 704-717, doi:10.1016/j.conbuildmat.2018.12.185.

[62] I. Skyrianou, L.N. Koutas, C.G. Papakonstantinou (2025). Metakaolin-based geopolymer mortars: Influence of mix design on mechanical properties and durability, Constr. Build. Mater., 490, 142526, doi:10.1016/j.conbuildmat.2025.142526.

[63] A. Naghizadeh, S.O. Ekolu, M. Welman-Purchase, L. Lagrange, L.N. Tchadjie (2025). Effective recycled binder produced upon thermal activation to enhance mechanical properties of fly ash-based geopolymer mortars, Dev. Built Environ., 23, 100688, doi:10.1016/j.dibe.2025.100688.

[64] M. Sun, Z. Li, Z. Li, Q. Xu, B. Zou, H. Liu, F. Wang (2025). Mechanical and microstructural properties of graphite tailings based geopolymer mortars at

high temperature, Case Stud. Constr. Mater., 23, e05388, doi:10.1016/j.cscm.2025.e05388.

[65] A. Erfanimanesh, M.K. Sharbatdar (2020). Mechanical and microstructural characteristics of geopolymer paste, mortar, and concrete containing local zeolite and slag activated by sodium carbonate, J. Build.Eng., 32, 101781, doi:10.1016/j.jobe.2020.101781.

[66] M. Ziada, H. Tanyildizi, A. Coskun (2025). Mechanical and microstructural properties of basalt fiber reinforced underwater geopolymer mortar, Structures, 75, 108814, doi:10.1016/j.istruc.2025.108814.

[67] K. Chen, D. Wu, M. Yi, Q. Cai, Z. Zhang (2021). Mechanical and durability properties of metakaolin blended with slag geopolymer mortars used for pavement repair, Constr. Build. Mater., 281, 122566, doi:10.1016/j.conbuildmat.2021.122566.

[68] Y. Yang, W. Zhou, Y. Yang, I. Mithal, X. Lu, Y. Zhang (2025). Fatigue behavior and microstructural mechanisms of fly ash-slag based geopolymer mortars under cyclic loading, Constr. Build. Mater., 494, 143236, doi:10.1016/j.conbuildmat.2025.143236.

[69] G. Fahim, M. Ismail, N. Hafizah, A. Khalid (2018). Compressive strength and microstructure of assorted wastes incorporated geopolymer mortars: Effect of solution molarity, Alexandria Eng. J., 57, 3375-3386, doi:10.1016/j.aej.2018.07.011.

[70] C. Ng, U.J. Alengaram, L. Sing, K. Hung, M. Zamin, S. Ramesh (2018). A review on microstructural study and compressive strength of geopolymer mortar, paste and concrete, Constr. Build.Mater., 186, 550-576, doi:10.1016/j.conbuildmat.2018.07.075.

[71] W. Huang, H. Wang (2024). Comprehensive assessment of engineering and environmental attributes of geopolymer pervious concrete with natural and recycled aggregate, J. Clean.Prod., 468, 143138, doi:10.1016/j.jclepro.2024.143138.

[72] K. Walbruck, L. Drewler, S. Witzleben, D. Stephan (2021).Factors influencing thermal conductivity and compressive strength of natural fiber-reinforced geopolymer foams, Open Ceram., 5, 100065, doi:10.1016/j.oceram.2021.100065.

[73] B. Bayrak, A. Benli, H.G. Alcan, O. Celebi, G. Kaplan, A.C. Aydin (2023). Recycling of waste marble powder and waste colemanite in ternary-blended green geopolymer composites: Mechanical, durability and microstructural properties, J. Build.Eng., 73, 106661, doi:10.1016/j.jobe.2023.106661.

[74] M.S. Saif, M.O.R. El-Hariri, A.I. Sarie-Eldin, B.A. Tayeh, M.F. Farag (2022). Impact of Ca+ content and curing condition on durability performance of metakaolin-based geopolymer mortars, Case Stud. Constr. Mater., 16, e00922, doi:10.1016/j.cscm.2022.e00922.

[75] A.R. Villca, F. Vargas, J. Araya, L. Rojas, C. Villarroel (2021). Lime/pozzolan/geopolymer systems: Performance in pastes and mortars, Constr. Build. Mater., 276, 122208, doi:10.1016/j.conbuildmat.2020.122208.

[76] F. Longo, P. Lassandro, A. Moshiri, T. Phatak, M.A. Aiello, K.J. Krakowiak (2020). Lightweight geopolymer-based mortars for the structural and energy retrofit of buildings, Energy Build., 225, 110352, doi:10.1016/j.enbuild.2020.110352.

[77] Z. Sun, A. Vollpracht (2020). Leaching of monolithic geopolymer mortars, Cem.Concr.Res., 136, 106161, doi:10.1016/j.cemconres.2020.106161.

[78] A. Lo Bianco, F. Armetta, M.M. Calvino, G.E. Gagliardo Briuccia, B. Macalik, D. Hreniak, M.L. Saladino, G. Lazzara, G. Cavallaro (2026). Invisible near-infrared luminescent marker incorporating Egyptian blue in halloysite-based geopolymer mortars: Applications in covert tagging, J. Alloys Compd., 1050, 185458, doi:10.1016/j.jallcom.2025.185458.

[79] B.B. Jindal (2019). Investigations on the properties of geopolymer mortar and concrete with mineral admixtures: A review, Constr. Build. Mater., 227, 116644, doi:10.1016/j.conbuildmat.2019.08.025.

[80] I. Tank, S.K. Sharma, A. Goyal (2026). Investigation on fly ash-based geopolymer mortar: Effect of mix proportions and curing conditions on mechanical properties and durability characteristics of optimized mix, Next Mater., 10, 101565, doi:10.1016/j.nxmate.2025.101565.

[81] H. Liu, X. Dai, P. Zhu, X. Wang, M. Zong, J. Feng (2024). Acid rain resistance of geopolymer recycled pervious concrete featuring top-bottom interconnected pores under freeze-thaw cycles and fatigue loads, J. Build. Eng., 96, 110356, doi:10.1016/j.jobe.2024.110356.

[82] Z. Gao, P. Zhang, J. Wang, K. Wang, T. Zhang (2022). Interfacial properties of geopolymer mortar and concrete substrate: Effect of polyvinyl alcohol fiber and nano-SiO2 contents, Constr. Build. Mater., 315, 125735, doi:10.1016/j.conbuildmat.2021.125735.

[83] A.K. Kaya, M.I. Onur (2025). Optimization of physical, mechanical and thermal properties of two-part geopolymer mortar by Taguchi method, Constr. Build.Mater., 476, 141208, doi:10.1016/j.conbuildmat.2025.141208.

[84] P.W. Ariyadasa, A.C. Manalo, W. Lokuge, V. Aravinthan, A. Gerdes, J. Kaltenbach (2025). Degradation mechanisms of low-calcium fly ash-based geopolymer mortar in simulated aggressive sewer conditions, Cem.Concr.Res., 194, 107882, doi:10.1016/j.cemconres.2025.107882.

[85] P. Zhang, Y. Zheng, K. Wang, J. Zhang (2018). A review on properties of fresh and hardened geopolymer mortar, Compos. Part B Eng., 152, 79-95, doi:10.1016/j.compositesb.2018.06.031.

[86] G. Silva, S. Kim, B. Bertolotti, J. Nakamatsu, R. Aguilar (2020). Optimization of a reinforced geopolymer composite using natural fibers and construction wastes, Constr. Build.Mater., 258, 119697, doi:10.1016/j.conbuildmat.2020.119697.

[87] P. Zhu, X. Chen, H. Liu, Z. Wang, C. Chen, H. Li (2024). Recycling of waste recycled aggregate concrete in freeze-thaw environment and emergy

analysis of concrete recycling system, J. Build.Eng., 96, 110377, doi:10.1016/j.jobe.2024.110377.

[88] T. Bezabih, D. Sinkhonde, D. Mirindi, S. Kiprop, F. Mirindi, O. Abiodun (2025). Effects of mix design parameters on workability and compressive strength of teff straw ash-based geopolymer mortars: Experimental evaluation and machine learning prediction, Constr. Build. Mater., 502, 144487, doi:10.1016/j.conbuildmat.2025.144487.

[89] N. Bheel, P. Awoyera, T. Tafsirojjaman, N.H. Sor, S. Sohu (2021). Synergic effect of metakaolin and groundnut shell ash on the behavior of fly ash-based self-compacting geopolymer concrete, Constr. Build.Mater., 311, 125327, doi:10.1016/j.conbuildmat.2021.125327.

[90] A. Raza, B. Ahmed, M.H. El Ouni, W. Chen (2024). Mechanical, durability and microstructural characterization of cost-effective polyethylene fiber-reinforced geopolymer concrete, Constr. Build.Mater., 432, 136661, doi:10.1016/j.conbuildmat.2024.136661.

[91] H. Altawil (2025). Influence of saline exposure and freeze-thaw effects on class C fly ash geopolymer mortars using the Taguchi method, Results Eng., 27, 106836, doi:10.1016/j.rineng.2025.106836.

[92] T. Cakmak, I. Ustabas, E. Yilmaz (2025). Integrating obsidian and silica fume in geopolymer mortars: Strength prediction via meta-ensemble machine learning framework, Dev. Built Environ., 24, 100820, doi:10.1016/j.dibe.2025.100820.

[93] G. Ogwang, P.W. Olupot, H. Kasedde, E. Menya, H. Storz, Y. Kiros (2021). Experimental evaluation of rice husk ash for applications in geopolymer mortars, J. Bioresour. Bioprod., 6, 160-167, doi:10.1016/j.jobab.2021.02.008.

[94] L. Masoud, A. Hammoud, Y. Mortada, E. Masad (2024). Rheological, mechanical, and microscopic properties of polypropylene fiber reinforced-geopolymer concrete for additive manufacturing, Constr. Build. Mater., 438, 137069, doi:10.1016/j.conbuildmat.2024.137069.

[95] S. Kumar, S. Shrivastava (2021). Influence of molarity and alkali mixture ratio on ambient temperature cured waste cement concrete based geopolymer mortar, Constr. Build. Mater., 301, 124380, doi:10.1016/j.conbuildmat.2021.124380.

[96] R. Vijayalakshmi (2021). Recent studies on the properties of pervious concrete: A sustainable solution for pavements and water treatment, Civ. Environ. Eng. Rep., 31, 54-84, doi:10.2478/ceer-2021-0034.

[97] R.A. Mahmood, E. Delik, N.U. Kockal, B.E. Tefon-Ozturk (2025). Performance of bio-geopolymer mortar incorporation isolates of Bacillus cereus and Bacillus subtilis: A comprehensive experimental study, Next Mater., 8, 100845, doi:10.1016/j.nxmate.2025.100845.

[98] M. Saba, J.J. Assaad (2021). Effect of recycled fine aggregates on performance of geopolymer masonry mortars, Constr. Build. Mater., 279, 122461, doi:10.1016/j.conbuildmat.2021.122461.

[99] Z. Huang, J. Ling, J. Zhang, J. Li, H. Yang, Y. Zheng (2026). Influence of functional admixtures on the strength and shrinkage of seawater sea sand geopolymer mortar, Constr. Build. Mater., 513, 145504, doi:10.1016/j.conbuildmat.2026.145504.

[100] A.S. Bature, M. Khorami, E. Ganjian, M. Tyrer (2021). Influence of alkali activator type and proportion on strength performance of calcined clay geopolymer mortar, Constr. Build. Mater., 267, 120446, doi:10.1016/j.conbuildmat.2020.120446.

[101] Z. Sun, X. Lin, A. Vollpracht (2018). Pervious concrete made of alkali activated slag and geopolymers, Constr. Build. Mater., 189, 797-803, doi:10.1016/j.conbuildmat.2018.09.067.

[102] M. Jin, Z. Wang, F. Lian, P. Zhao (2020).Freeze-thaw resistance and seawater corrosion resistance of optimized tannery sludge/metakaolin-based geopolymer, Constr. Build.Mater., 265, 120730, doi:10.1016/j.conbuildmat.2020.120730.

[103] L. Niu, X. Nie, N. Li, J. Guan, L. Li, C. Xie (2026). Experimental and theoretical investigation of fiber-reinforced geopolymer mortars: Mix design optimization and bond behavior with brick masonry, Case Stud. Constr. Mater., 24, e05767, doi:10.1016/j.cscm.2026.e05767.

[104] E.K. Mermerdas, Z. Algin (2020).Experimental assessment and optimization of mix parameters of fly ash-based lightweight geopolymer mortar with respect to shrinkage and strength, J. Build.Eng., 31, 101351, doi:10.1016/j.jobe.2020.101351.

[105] H. Hamisi, S.T. Chambua, S. Mansouri, H. Majdoubi (2025).Compressive strength optimization of the ambient-cured metakaolin-based geopolymer mortar using the Taguchi design approach, Constr. Build.Mater., 475, 141248, doi:10.1016/j.conbuildmat.2025.141248.

[106] D. Huang, C. Lin, Z. Liu, Y. Lu, S. Li (2024). Compressive behaviors of steel fiber-reinforced geopolymer recycled aggregate concrete-filled GFRP tube columns, Structures, 66, 106829, doi:10.1016/j.istruc.2024.106829.

[107] H. Baykara, M.H. Cornejo, E. Garcia, N. Ulloa (2020). Preparation, characterization, and evaluation of compressive strength of polypropylene fiber reinforced geopolymer mortars, Heliyon, 6, e03755, doi:10.1016/j.heliyon.2020.e03755.

[108] M. Upshaw, C.S. Cai (2021). Feasibility study of MK-based geopolymer binder for RAC applications: Effects of silica fume and added CaO on compressive strength of mortar samples, Case Stud. Constr. Mater., 14, e00500, doi:10.1016/j.cscm.2021.e00500.

[109] A. Grinys, M. Statkauskas (2025).Effect of elevated temperature on mechanical properties of ceramic brick and metakaolin waste-based geopolymer mortar, Constr. Build.Mater., 470, 140431, doi:10.1016/j.conbuildmat.2025.140431.

[110] P. Yoosuk, C. Suksiripattanapong, P. Sukontasukkul (2021). Properties of polypropylene fiber reinforced cellular lightweight high calcium fly ash geopolymer mortar, Case Stud. Constr. Mater., 15, e00730, doi:10.1016/j.cscm.2021.e00730.

[111] P. Darvish, U.J. Alengaram, A. Mahmoud, Y. Soon, S. Ibrahim (2021). Enunciation of size effect of sustainable palm oil clinker sand on the characteristics of cement and geopolymer mortars, J. Build.Eng., 44, 103335, doi:10.1016/j.jobe.2021.103335.

[112] X. Liang, Y. Ji (2021).Experimental study on durability of red mud-blast furnace slag geopolymer mortar, Constr. Build.Mater., 267, 120942, doi:10.1016/j.conbuildmat.2020.120942.

[113] T.H. Vu, N. Gowripalan, P. De Silva, A. Paradowska, U. Garbe, P. Kidd, V. Sirivivatnanon (2020). Assessing carbonation in one-part fly ash/slag geopolymer mortar: Change in pore characteristics using the state-of-the-art technique neutron tomography, Cem. Concr.Compos., 114, 103759, doi:10.1016/j.cemconcomp.2020.103759.

[114] L. Hong, W. Tang, Y. Tan, Y. Wang, B. Guo, P. Gao (2025). Effect of short fibers on non-uniform strain distribution of geopolymer mortar under dry conditions, Constr. Build.Mater., 459, 139768, doi:10.1016/j.conbuildmat.2024.139768.

[115] P. Duxson, J.L. Provis, G.C. Lukey, J.S.J. van Deventer (2007).The role of inorganic polymer technology in the development of green concrete, Cem.Concr.Res., 37, 1590-1597, doi:10.1016/j.cemconres.2007.08.018.

[116] Z. Jiao, X. Li, Q. Yu (2021).Effect of curing conditions on freeze-thaw resistance of geopolymer mortars containing various calcium resources, Constr. Build.Mater., 313, 125507, doi:10.1016/j.conbuildmat.2021.125507.

[117] H. Zhang, J. Liu, B. Wu (2021).Mechanical properties and reaction mechanism of one-part geopolymer mortars, Constr. Build.Mater., 273, 121973, doi:10.1016/j.conbuildmat.2020.121973.

[118] G.A. Ramos, P.R. de Matos, F. Pelisser, P.J.P. Gleize (2020). Effect of porcelain tile polishing residue on eco-efficient geopolymer: Rheological performance of pastes and mortars, J. Build. Eng., 32, 101699, doi:10.1016/j.jobe.2020.101699.

IZVOD

OPTIMIZACIJA GEOPOLIMERNOG MALTERA NA BAZI LETEĆEG PEPELA AKTIVIRANOG ALKALIJAMA: UTICAJ SASTAVA AKTIVATORA NA ČVRSTOĆU I OBRADIVOST

U ovoj studiji istražuje se uticaj sastava alkalijskog aktivatora, sadržaja vode i proporcija mešavine na obradivost u svežem stanju, mehanička svojstva i mikrostrukturu geopolimernih maltera na bazi letećeg pepela. Pripremljeno je ukupno 40 mešavina geopolimernih maltera, a za svaku mešavinu su testirana tri ponovljena uzorka. Sve mešavine su proizvedene sa konstantnim odnosom peska i letećeg pepela od 2:1, dok je molarnost natrijum hidroksida (NaOH) varirala na 8 M, 12 M, 14 M i 16 M, a odnos natrijum silikata i NaOH (SS/NaOH) kretao se od 0,1 do 2,5. Sadržaj vode varirao je od 1 do 8% po težini letećeg pepela za fiksne odnose rastvora i veziva od 0,4 i 0,5. Uzorci su očvršćeni na 85°C tokom 24 sata u peći radi olakšavanja geopolimerizacije. Obradivost je procenjena pomoću testa tečnosti, a vrednosti tečenja su se kretale između 120% i 140%. Čvrstoća na pritisak je određena u starosti očvršćavanja od 3, 7 i 28 dana. Maksimalna čvrstoća na pritisak od 68 MPa dobijena je pri koncentraciji NaOH od 16 M i odnosu SS/NaOH od 1,5. Ovaj optimalni sastav odgovara odnosu Na_2O/SiO_2 u opsegu od 0,15–0,17, što ukazuje da oba parametra opisuju istu optimalnu hemiju aktivatora izraženu korišćenjem različitih formata odnosa. Analiza rendgenske difrakcije (XRD) otkrila je formiranje zeolitnih faza tipa hidroksisodalita pri višim odnosima SS/NaOH, što doprinosi poboljšanom razvoju čvrstoće. Povećanje odnosa H_2O/Na_2O iznad 0,22 rezultiralo je smanjenjem čvrstoće zbog povećane poroznosti. Rezultati identifikuju kritične opsege sadržaja aktivatora i vode koji omogućavaju efikasnu ravnotežu između obradivosti i čvrstoće na pritisak, pružajući kvantitativnu osnovu za optimizaciju proporcija mešavine maltera na bazi letećeg pepela aktiviranih alkalijama.

Ključne reči: *Geopolimerni malter. alkalna aktivacija, čvrstoća na pritisak, reologija i obradivost. fazna transformacija*

Naučni rad
Rad primljen: 29.01.2025.
Rad korigovan: 25.02.2026.
Rad prihvaćen: 8.03.2026

Sathia Ramalingam: https://orcid.org/0000-0002-0851-2145
Vijayalakshmi Ramalingam: https://orcid.org/0000-0003-4678-2020
Aswin Sriram: https://orcid.org/0000-0001-7416-8605